

**FINAL DATA REPORT  
Revision 0  
GEOTECHNICAL EXPLORATION AND TESTING  
SUPPLEMENT 2  
DOMINION POWER  
NORTH ANNA NUCLEAR POWER STATION  
NORTH ANNA 3 PROJECT  
MINERAL, LOUISA COUNTY, VIRGINIA**

**December 16, 2009**

**VOLUME 1**

**APPENDIX C.1  
Geovision Downhole and P-S Logging Report**

**Prepared By:**

**MACTEC ENGINEERING AND CONSULTING, INC.  
RALEIGH, NORTH CAROLINA**

**MACTEC PROJECT No. 6468-09-2473**

**Prepared For:**

**Bechtel Power Corporation  
Subcontractor No. 25161-500-HC4-CY00-00001**



DOCUMENTATION OF TECHNICAL REVIEW  
SUBCONTRACTOR WORK PRODUCT

Project Name: NORTH ANNA 3 PROJECT

Project Number: 6468-09-2473

Project Manager: Steve Criscenzo

Project Principals: Al Tice and Steve Copley

The report described below has been prepared by the named subcontractor retained in accordance with the MACTEC QAPD. The work and report have been reviewed by a MACTEC technically qualified person. Comments on the work or report, if any, have been satisfactorily addressed by the subcontractor. The attached report is approved in accordance with section QS-7 of MACTEC's QAPD

The information and date contained in the attached report are hereby released by MACTEC for project use.

REPORT :

North Anna Project 3 GEOVision Report, Revision 0 11-3-2009

---

SUBCONTRACTOR: GEOVision Geophysical Services

---

DATE OF ACCEPTANCE: 11-4-09

TECHNICAL REVIEWER:

PROJECT PRINCIPAL

DCN - NAP274



3301 Atlantic Avenue, Raleigh, NC 27604



## **FINAL REPORT**

### **BORING GEOPHYSICS BORINGS M-10DH AND M-30DH**

### **NORTH ANNA 3 PROJECT NORTH ANNA NUCLEAR STATION**

**Report 9333-01 rev 0**

**November 3, 2009**

**FINAL REPORT**

**BORING GEOPHYSICS**

**BORINGS M-10DH AND M-30DH**

**NORTH ANNA 3 PROJECT**

**NORTH ANNA NUCLEAR STATION**

**Report 9333-01 rev 0**

**November 3, 2009**

**Prepared for:**

**MACTEC Engineering and Consulting, Inc.**

**3301 Atlantic Avenue**

**Raleigh, N. C. 27604**

**919-876-0416**

**MACTEC Job number 6468-09-2473**

**Prepared by**

**GEOVision Geophysical Services**

**1124 Olympic Drive**

**Corona, California 92881**

**(951) 549-1234**

## TABLE OF CONTENTS

<b>TABLE OF CONTENTS</b> .....	<b>3</b>
<b>TABLE OF FIGURES</b> .....	<b>4</b>
<b>TABLE OF TABLES</b> .....	<b>4</b>
<b>INTRODUCTION</b> .....	<b>6</b>
<b>SCOPE OF WORK</b> .....	<b>6</b>
<b>INSTRUMENTATION</b> .....	<b>8</b>
SUSPENSION INSTRUMENTATION .....	8
CALIPER / NATURAL GAMMA INSTRUMENTATION .....	10
RESISTIVITY / SPONTANEOUS POTENTIAL / NATURAL GAMMA INSTRUMENTATION .....	12
ACOUSTIC TELEVIEWER / BORING DEVIATION INSTRUMENTATION .....	13
<b>MEASUREMENT PROCEDURES</b> .....	<b>16</b>
SUSPENSION MEASUREMENT PROCEDURES .....	16
CALIPER / NATURAL GAMMA MEASUREMENT PROCEDURES .....	17
RESISTIVITY / SPONTANEOUS POTENTIAL MEASUREMENT PROCEDURES .....	18
ACOUSTIC TELEVIEWER / BORING DEVIATION MEASUREMENT PROCEDURES .....	20
<b>DATA ANALYSIS</b> .....	<b>21</b>
SUSPENSION ANALYSIS .....	21
CALIPER / NATURAL GAMMA ANALYSIS .....	23
RESISTIVITY / NATURAL GAMMA / SPONTANEOUS POTENTIAL ANALYSIS .....	23
ACOUSTIC TELEVIEWER / BORING DEVIATION ANALYSIS .....	24
<b>RESULTS</b> .....	<b>25</b>
SUSPENSION RESULTS .....	25
CALIPER/ NATURAL GAMMA RESULTS .....	26
RESISTIVITY / SPONTANEOUS POTENTIAL RESULTS .....	26
ACOUSTIC TELEVIEWER / BORING DEVIATION RESULTS .....	26
<b>SUMMARY</b> .....	<b>28</b>
DISCUSSION OF SUSPENSION RESULTS .....	28
DISCUSSION OF CALIPER / NATURAL GAMMA RESULTS .....	29
DISCUSSION OF RESISTIVITY / SPONTANEOUS POTENTIAL RESULTS .....	29
DISCUSSION OF ACOUSTIC TELEVIEWER / BORING DEVIATION RESULTS .....	29
QUALITY ASSURANCE .....	30
SUSPENSION DATA RELIABILITY .....	31

## Table of Figures

Figure 1: Concept illustration of P-S logging system .....	32
Figure 2. Example Calibration Curve for Caliper Probe.....	33
Figure 3: Example of filtered (1400 Hz lowpass) record.....	36
Figure 4. Example of unfiltered record .....	37
Figure 5: Boring M-10DH, Suspension R1-R2 P- and S <sub>H</sub> -wave velocities.....	38
Figure 6: Boring M-10DH, Caliper, Natural gamma, Resistivity and SP logs.....	42
Figure 7. Boring M-10DH, Deviation Projection .....	43
Figure 8: Boring M-30DH, Suspension R1-R2 P- and S <sub>H</sub> -wave velocities.....	44
Figure 9. Boring M-30DH, Caliper, Natural gamma, Resistivity and SP logs.....	48
Figure 10. Boring M-30DH, Deviation Projection.....	49

## Table of Tables

Table 1 Boring locations and logging dates.....	34
Table 2. Logging dates and depth ranges .....	34
Table 3. Boring Bottom Depths and After Survey Depth Error (ASDE).....	35
Table 4. Boring Deviation Data Summary.....	35
Table 5. Boring M-10DH, Suspension R1-R2 depths and P- and S <sub>H</sub> -wave velocities .....	39
Table 6. Boring M-30DH, Suspension R1-R2 depths and P- and S <sub>H</sub> -wave velocities .....	45

## **APPENDICES**

- APPENDIX A      SUSPENSION VELOCITY MEASUREMENT COMPARISON  
OF SOURCE TO RECEIVER 1 AND RECEIVER 1 TO  
RECEIVER 2 ANALYSIS RESULTS**
- APPENDIX B      CALIPER, NATURAL GAMMA, RESISTIVITY, AND  
SPONTANEOUS POTENTIAL LOGS**
- APPENDIX C      ACOUSTIC TELEVIEWER DIP LOGS**
- APPENDIX D      GEOPHYSICAL LOGGING SYSTEMS - NIST TRACEABLE  
CALIBRATION PROCEDURES AND CALIBRATION RECORDS**
- APPENDIX E      BORING GEOPHYSICAL LOGGING FIELD DATA LOGS**
- APPENDIX F      BORING GEOPHYSICAL LOGGING FIELD MEASUREMENT  
PROCEDURES**

## INTRODUCTION

Boring geophysical measurements were collected in two uncased borings located at the North Anna Nuclear Power Station, located in Louisa County, Virginia. Geophysical data acquisition was performed between September 15 and 17, 2009 by Charles Carter and Victor Gonzalez of **GEOVision**. Data analysis and report preparation were performed by Robert Steller and reviewed by John Diehl of **GEOVision**. The work was performed under subcontract with MACTEC Engineering and Consulting, Inc., (MACTEC) with J. Allan Tice serving as the point of contact for MACTEC.

This report describes the field measurements, data analysis, and results of this work.

## SCOPE OF WORK

This report presents the results of boring geophysical measurements collected between September 15 and 17, 2009, in two uncased borings, as detailed in Table 1. The purpose of these studies was to supplement stratigraphic information obtained during MACTEC's soil and rock sampling program and to acquire shear wave velocities and compressional wave velocities as a function of depth.

The OYO Suspension PS Logging System was used to obtain in-situ horizontal shear and compressional wave velocity measurements at 1.6 foot intervals. The acquired data were analyzed and a profile of velocity versus depth was produced for both compressional and horizontally polarized shear waves.

A Robertson Geologging 3ACS 3-arm mechanical caliper probe was used to collect boring diameter and natural gamma data at 0.05 foot intervals.

A Robertson Geologging ELXG probe was used to collect long and short normal resistivity, single point resistance, self potential, and natural gamma data at 0.05 foot intervals.

A Robertson Geologging High Resolution Acoustic Televierer (HiRAT) probe was used to collect Acoustic televierer images of the boring walls, and boring deviation data, at 0.008 foot intervals.

A detailed reference for the velocity measurement techniques used in this study is:

Guidelines for Determining Design Basis Ground Motions, Report TR-102293,  
Electric Power Research Institute, Palo Alto, California, November 1993,  
Sections 7 and 8.

## INSTRUMENTATION

### Suspension Instrumentation

Suspension soil and rock velocity measurements were performed using the suspension PS logging system, manufactured by OYO Corporation. This system directly determines the average in-situ horizontal shear and compressional wave velocity measurements of a 3.3 foot high segment of the rock and soil column surrounding the boring of interest by measuring the elapsed time between arrivals of a wave propagating upward through the rock and soil column. The receivers that detect the wave, and the source that generates the wave, are moved as a unit in the boring producing relatively constant amplitude signals at all depths.

The suspension system probe consists of a combined reversible polarity solenoid horizontal shear-wave source ( $S_H$ ) and compressional-wave source (P), joined to two biaxial receivers by a flexible isolation cylinder, as shown in Figure 1. The separation of the two receivers is 3.3 feet, allowing average wave velocity in the region between the receivers to be determined by inversion of the wave travel time between the two receivers. The total length of the probe as used in these surveys is 19 feet, with the center point of the receiver pair 12.1 feet above the bottom end of the probe.

The probe receives control signals from, and sends the digitized receiver signals to, instrumentation on the surface via an armored 4 conductor cable. The cable is wound onto the drum of a winch and is used to support the probe. Cable travel is measured to provide probe depth data, using a 3.28 foot circumference sheave fitted with a digital rotary encoder.

The entire probe is suspended in the boring by the cable, therefore, source motion is not coupled directly to the boring walls; rather, the source motion creates a horizontally propagating impulsive pressure wave in the fluid filling the boring and surrounding the source. This pressure wave is converted to P and  $S_H$ -waves in the surrounding soil and rock as it impinges upon the wall of the boring. These waves propagate through the soil and rock surrounding the boring, in

turn causing a pressure wave to be generated in the fluid surrounding the receivers as the soil waves pass their location. Separation of the P and  $S_H$ -waves at the receivers is performed using the following steps:

1. Orientation of the horizontal receivers is maintained parallel to the axis of the source, maximizing the amplitude of the recorded  $S_H$  -wave signals.
2. At each depth,  $S_H$ -wave signals are recorded with the source actuated in opposite directions, producing  $S_H$ -wave signals of opposite polarity, providing a characteristic  $S_H$ -wave signature distinct from the P-wave signal.
3. The 6.3 foot separation of source and receiver 1 permits the P-wave signal to pass and damp significantly before the slower  $S_H$ -wave signal arrives at the receiver. In faster soils or rock, the isolation cylinder is extended to allow greater separation of the P- and  $S_H$ -wave signals.
4. In saturated soils, the received P-wave signal is typically of much higher frequency than the received  $S_H$ -wave signal, permitting additional separation of the two signals by low pass filtering.
5. Direct arrival of the original pressure pulse in the fluid is not detected at the receivers because the wavelength of the pressure pulse in fluid is significantly greater than the dimension of the fluid annulus surrounding the probe (meter versus centimeter scale), preventing significant energy transmission through the fluid medium.

In operation, a distinct, repeatable pattern of impulses is generated at each depth as follows:

1. The source is fired in one direction producing dominantly horizontal shear with some vertical compression, and the signals from the horizontal receivers situated parallel to the axis of motion of the source are recorded.
2. The source is fired again in the opposite direction and the horizontal receiver signals are recorded.
3. The source is fired again and the vertical receiver signals are recorded. The repeated source pattern facilitates the picking of the P and  $S_H$ -wave arrivals; reversal of the source changes the polarity of the  $S_H$ -wave pattern but not the P-wave pattern.

The data from each receiver during each source activation are recorded as a different channel on the recording system. The Suspension PS system has six channels (two simultaneous recording channels), each with a 1024 sample record. The recorded data are displayed as six channels with a common time scale. Data are stored on disk for further processing. Up to 8 sampling sequences can be summed to improve the signal to noise ratio of the signals.

Review of the displayed data on the recorder or computer screen allows the operator to set the gains, filters, delay time, pulse length (energy), sample rate, and summing number to optimize the quality of the data before recording. Verification of the calibration of the Suspension PS digital recorder is performed every twelve months using a NIST traceable frequency source and counter, as outlined in Appendix D. An additional post-project calibration was performed following the field work, and is included in Appendix D.

### **Caliper / Natural Gamma Instrumentation**

Caliper and natural gamma data were collected using a Model 3ACS 3-leg caliper probe, serial number 6621, manufactured by Robertson Geologging, Ltd. With the short arm configuration used in these surveys, the probes permitted measurement of boring diameters between 1.6 and 12 inches. With this tool, caliper measurements were collected concurrent with measurement of natural gamma emission from the boring walls. The probe was 6.82 feet long, and 1.5 inches in diameter.

This probe is useful in the following studies:

- Measurement of boring diameter and volume
- Location of hard and soft formations
- Location of fissures, caving, pinching and casing damage
- Bed boundary identification
- Strata correlation between borings

The probe receives control signals from, and sends the digitized measurement values to, a Robertson Micrologger II on the surface via an armored 4 conductor cable. The cable is wound onto the drum of a winch and is used to support the probe. Cable travel is measured to provide probe depth data, using a 3.28 foot circumference sheave fitted with a digital rotary encoder. The probe and depth data are transmitted by USB link from the Micrologger unit to a laptop computer where it is displayed and stored on hard disk.

The caliper consists of three arms, each with a toothed quadrant at their base, pivoted in the lower probe body. A toothed rack engages with each quadrant, thus constraining the arms to move together. Linear movement of the rack is converted to opening and closing of the arms. Springs hold the arms open in the operating position. A motor drive is provided to retract the arms, allowing the probe to be lowered into the boring. The rack is coupled to a potentiometer which converts movement into a voltage sensed by the probe's microprocessor.

Natural gamma measurements rely upon small quantities of radioactive material contained in all rocks to emit gamma radiation as they decay. Trace amounts of Uranium and Thorium are present in a few minerals, whereas potassium-bearing minerals such as feldspar, mica and clays will include traces of a radioactive isotope of Potassium. These emit gamma radiation as they decay with an extremely long half-life. This radiation is detected by scintillation - the production of a tiny flash of light when gamma rays strike a crystal of sodium iodide. The light is converted into an electrical pulse by a photomultiplier tube. Pulses above a threshold value of 60 KeV are counted by the probe's microprocessor. The measurement is useful because the

radioactive elements are concentrated in certain rock types e.g. clay or shales, and depleted in others e.g. sandstone or coal.

## **Resistivity / Spontaneous Potential / Natural Gamma Instrumentation**

Resistivity, spontaneous potential and natural gamma data were collected using a Model ELXG electric log probe, S/N 5490, manufactured by Robertson Geologging, Ltd. This probe measures Single Point Resistance (SPR), short normal (16") resistivity, long normal (64") resistivity, Spontaneous Potential (SP) and natural gamma. The probe is 8.20 feet long, and 1.73 inches in diameter.

This probe is useful in the following studies:

- Bed boundary identification
- Strata correlation between borings
- Strata geometry and type (shale indication)

The probe receives control signals from, and sends the digitized measurement values to, a Robertson Micrologger II on the surface via an armored 4 conductor cable. The cable is wound onto the drum of a winch and is used to support the probe. Cable travel is measured to provide probe depth data, using a 3.28 foot circumference sheave fitted with a digital rotary encoder. The probe and depth data are transmitted by USB link from the Micrologger unit to a laptop computer where they are displayed and stored on hard disk.

The resistivity section of the probe operates by driving an alternating current into the formation from the central SPR/DRIVE electrode. The current returns via the logging cable armor. To ensure adequate penetration of the formation the logging cable is insulated for approximately 30 feet from the cablehead. Voltages are measured between the 16" and 64" electrodes and the remote earth connection at surface, as noted below:

- Single Point Resistance (SPR): The current flowing to the cable armor is measured along with the voltage at the SPR electrode. The voltage divided by current gives resistance.
- Self Potential (SP): This is the DC bias of the 16" electrode with respect to the voltage return at the surface (ground stake).

Data quality is dependant upon good grounding at the surface. This is achieved with a metal stake driven into the mud-pit or the soil adjacent to the boring.

### **Acoustic Televierer / Boring Deviation Instrumentation**

An acoustic image and boring deviation data were collected in all three borings using a High Resolution Acoustic Televierer probe (HiRAT), serial number 6641, manufactured by Robertson Geologging, Ltd. The probe is 7.58 feet long, and 1.9 inches in diameter, and is fitted with upper and lower four-band centralizers.

In this application, this probe is useful in the following studies:

- Measurement of boring inclination and deviation from vertical
- Determination of need to correct soil and geophysical log depths to true vertical depths
- Acoustic imaging of the boring wall to identify fractures, dikes, and weathered zones, and determine dip and azimuth of these features

The probe receives control signals from, and sends the digitized measurement values to, a Robertson Micrologger II on the surface via an armored 4 conductor cable. The cable is wound onto the drum of a winch and is used to support the probe. Cable travel is measured to provide probe depth data, using a 3.28 foot circumference sheave fitted with a digital rotary encoder. The probe and depth data are transmitted by USB link from the Micrologger unit to a laptop computer where it is displayed and stored on hard disk.

This system produces images of the boring wall based upon the amplitude and travel time of an ultrasonic beam reflected from the formation wall. The ultrasonic energy is generated by a piezoelectric transducer at a frequency of 1.4 MHz. A periodic acoustic energy wave is emitted by the transducer and travels through the acoustic head and boring fluid until it reaches the interface between the boring fluid and the boring wall. Here a portion of the energy is reflected back to the transducer, the remainder continuing on into the formation. By careful time sequencing, the piezoelectric transducer acts as both the transmitter of the ultrasonic pulse and receiver of the reflected wave. The travel time of the energy wave is the period between transmission of the source energy pulse and the return of the reflected wave measured at the point of maximum wave amplitude. The magnitude of the wave energy is measured in dB, a unit-less ratio of the detected echo wave amplitude divided by the amplitude of the transmitted wave. The strength of the reflected signal depends primarily upon the impedance contrast of the boring fluid and the boring wall formation. In these rock borings, the contrast between the clear water filling the boring and the rock formation generally provides high contrast. The changes in contrast between native rock and dikes provide imaging of fracture fillings.

The acoustic wave propagates along the axis of the probe and then is reflected perpendicular to this axis by a reflector that focuses the beam to a 0.1-inch diameter spot about 2 inches from the central axis of the probe. This reflector is mounted on the shaft of a stepper motor enabling the position of the measurement to be rotated through 360°. Sampling rates of 90, 180 and 360 measured points per revolution are available. During these surveys, data were collected at 360 samples per revolution. It should be noted that during logging the probe is moving in the boring, so that the measured points describe a very fine pitch spiral.

The probe contains a fluxgate magnetometer to monitor magnetic north, and all raw televiewer data are referenced to magnetic north. Also, a three-axis accelerometer is enclosed in the probe, and boring deviation data are recorded during the logging runs, to permit correction of structure dip angle from apparent dip, (referenced to boring axis), to true dip (referenced to a vertical axis) in non-vertical borings.

The data are presented on a computer screen for operator review during the logging run, and stored on hard disk for later processing.

## MEASUREMENT PROCEDURES

### Suspension Measurement Procedures

The borings were filled with bentonite or polymer based drilling mud and logged from the bottom of the surface casing down to the bottom of the boring, as listed in Table 2. 4-inch steel casing placed in the top 44 to 90 feet of softer soils above bedrock contact during the measurements in the lower rock portion of the borings. The casing was then removed, and measurements were performed in the upper soil portion of the borings, as indicated in Table 2. Measurements followed the **GEOVision** Procedure for P-S Suspension Seismic Velocity Logging, revision 1.4, as presented in Appendix F. This procedure was supplied to and approved by MACTEC in advance of the work. In each boring, the probe was positioned with the top of the probe at the top of the casing, and the electronic depth counter was set to the specified length of the probe, minus the height of the casing stick-up, as verified with a tape measure, and recorded on the field logs. The probe was lowered to the bottom of the boring, stopping at 1.6 foot intervals to collect data, as summarized in Table 2.

At each measurement depth the measurement sequence of two opposite horizontal records and one vertical record was performed, and the gains were adjusted as required. The data from each depth was reviewed on the computer display, and recorded on disk before moving to the next depth.

Upon completion of the measurements, the probe zero depth indication at the depth reference point was verified prior to removal from the boring, and the after survey depth error (ASDE) was calculated, as summarized in Table 3.

Calibration procedures and records for the suspension PS measurement system are presented in Appendix D. **GEOVision** standard field log sheets for all borings are reproduced in Appendix E and **GEOVision** standard field procedures are reproduced in Appendix F.

## Caliper / Natural Gamma Measurement Procedures

The borings were filled with bentonite or polymer based drilling mud and logged from the bottom of the boring up until the caliper entered the bottom of the surface casing, as listed in Table 2. Measurements followed ASTM D6167-97 (Re-approved 2004) Conducting Borehole Geophysical Logging – Mechanical Caliper.

Prior to and following each logging run, the caliper tool was verified, using the manufacturer's supplied three point calibration jig, and a PVC coupling provided by MACTEC with an inside diameter traceable to NIST. The three point jig is a circular plate with a series of holes in the top surface into which the tips of the caliper arms fit. This has circles of diameters from 2 to 12 inches. The calibration jig is placed over a bucket with the probe standing upright with its nose section passing through the jig's central hole. The caliper probe arms are opened under program control, and a log is recorded as the tips of the arms are placed in the holes on the calibration jig and inside the PVC coupling. The measured dimensions, as displayed on the recording computer screen was recorded on the field log sheet, as well as in the digital files, and compared with the calibration jig dimensions. These files are presented in LAS 2.0 format in the boring specific sub-directories of the data disk (CD-R) labeled Report 9333-02 that accompanies this report. If the verification records did not fall within +/- 0.05 inches of the calibration jig values, the caliper tool was re-calibrated, using the three point calibration jig, and the log repeated. As with the verification, the tips of the caliper arms are placed in the holes marked with the required diameter. During calibration, the value of the current calibration point, as stamped on the jig, is entered via the control computer. The system counts for 15 seconds to make an average of the response. The procedure is repeated for the second and third required openings.

The computation and generation of the calibration coefficient file is entirely automatic. The calibration file is simply the set of coefficients of a quadratic curve which fits the three data points. Figure 2 shows the response of a caliper probe using data gathered during calibration.

Natural gamma was not calibrated in the field, as it is a qualitative measurement, not a quantitative value, and is used only to assist in picking transitions between stratigraphic units, as

described in ASTM D6274-98 (Re-approved 2004), Conducting Borehole Geophysical Logging - Gamma.

In each boring, the probe was positioned with the top of the probe at the top of the casing, and the electronic depth counter was set to the specified length of the probe, minus the height of the casing stick-up, as verified with a tape measure, and recorded on the field logs. The probe was lowered to the bottom of the boring, where the caliper legs were opened, and data collection begun. The probe was then returned to the surface at 10 feet/minute, collecting data continuously at 0.05 foot spacing, as summarized in Table 2.

Upon completion of the measurements, the probe zero depth indication at the depth reference point was verified prior to removal from the boring, and the after survey depth error (ASDE) was calculated, as summarized in Table 3.

### **Resistivity / Spontaneous Potential Measurement Procedures**

The borings were filled with bentonite or polymer based drilling mud and logged from the bottom of the boring up until the yoke electrode cleared the surface of the drilling mud at nominal 39 foot depth, or the probe entered the surface casing, as summarized in Table 2. The probe was connected to the logging cable using a 32.8 foot long insulating cable section or “yoke”. The probe head was insulated by wrapping all exposed metal of the cablehead and probe with self-amalgamating insulation tape. The 32.8 foot insulating yoke was checked for any damage, and repaired with self-amalgamating insulation tape as needed.

The reference ground stake was driven firmly into the mud pit, and connected to the ground socket on the winch switch box.

This sonde was not calibrated in the field, as it is used to provide qualitative measurements, not quantitative values, and is used only to assist in picking transitions between stratigraphic units, as described in ASTM D5753-05, Planning and Conducting Borehole Geophysical Surveys. A

functional test is performed prior to each logging run by applying fixed resistance values across the probe electrodes, as well as a 100 millivolt signal across the SP electrodes, and recording the resultant output of the system. These functional checks are presented in LAS 2.0 format in the boring specific sub-directories of the data directory on the data disk (CD-R) labeled Report 9333-02 that accompanies this report.

Natural gamma was not calibrated in the field, as it is a qualitative measurement, not a quantitative value, and is used only to assist in picking transitions between stratigraphic units, as described in ASTM D6274-98 (Re-approved 2004), Conducting Borehole Geophysical Logging - Gamma.

In each boring, the probe was positioned with the top of the yoke electrode at the top of the casing, and the electronic depth counter was set to the specified length of the probe and yoke, minus the height of the casing stick-up, as verified with a tape measure, and recorded in the field logs. The probe was lowered to the bottom of the boring, where data collection was begun. The probe was then returned to the surface at 10 feet/minute, collecting data continuously at 0.05 foot spacing, until the yoke electrode cleared the surface of the drilling mud at nominal 39 foot depth, or the probe entered the surface casing, as summarized in Table 2. The natural gamma data collected in these logs is redundant with the data collected in the caliper / natural gamma logs, and the caliper / natural data may be used to verify the natural gamma data collected in these logs.

Upon completion of the measurements, the probe zero depth indication at the depth reference point was verified prior to removal from the boring, and the after survey depth error (ASDE) was calculated, as summarized in Table 3.

## **Acoustic Televiwer / Boring Deviation Measurement Procedures**

The borings were filled with bentonite or polymer based drilling mud and logged from the bottom of the boring up to the surface, as listed in Table 2. Measurements followed the **GEOVision** Hi-RAT Field Procedure, revision 1.0, as presented in Appendix F. This procedure was supplied to and approved by MACTEC in advance of the work.

Prior to use, the HiRAT probe tiltmeter and compass functions were checked by comparison with a Brunton surveyors' compass, and the results recorded on the field logs.

In each boring, the televiwer probe was positioned with the top of the probe at the top of the casing, and the electronic depth counter was set to the specified length of the probe, minus the height of the casing stick-up, as verified with a tape measure, and recorded on the field logs. The probe was lowered to the bottom of the boring, and data collection begun. The probe was then returned to the surface at 3.0 feet/minute, collecting data continuously at 0.008 foot intervals, as summarized in Table 2.

Upon completion of the measurements, the probe zero depth indication at grade was verified prior to removal from the boring and the after survey depth error (ASDE) was calculated, as summarized in Table 3.

## DATA ANALYSIS

### Suspension Analysis

Using the proprietary OYO program PSLOG.EXE version 1.0, included on the data disk (CD-R) labeled Report 9333-02 that accompanies this report, the recorded digital waveforms were analyzed to locate the most prominent first minima, first maxima, or first break on the vertical axis records, indicating the arrival of P-wave energy. The difference in travel time between receiver 1 and receiver 2 (R1-R2) arrivals was used to calculate the P-wave velocity for that 3.3 foot segment of the soil column. When observable, P-wave arrivals on the horizontal axis records were used to verify the velocities determined from the vertical axis data. The time picks were then transferred into an EXCEL template (EXCEL version 2003 SP2) to complete the velocity calculations based upon the arrival time picks made in PSLOG. The PSLOG pick files and the EXCEL analysis files are included in the boring specific directories on the data disk (CD-R) labeled Report 9333-02 that accompanies this report.

The P-wave velocity over the 6.3 foot interval from source to receiver 1 (S-R1) was also picked using PSLOG, and calculated and plotted in EXCEL, for comparison with the velocity derived from the travel time between receivers. In this analysis, the depth values as recorded were increased by 4.8 feet to correspond to the mid-point of the 6.3 foot S-R1 interval. Travel times were obtained by picking the first break of the P-wave signal at receiver 1 and subtracting 0.3 milliseconds, the calculated and experimentally verified delay from source trigger pulse (beginning of record) to source impact. This delay corresponds to the duration of acceleration of the solenoid before impact.

As with the P-wave records, using PSLOG, the recorded digital waveforms were analyzed to locate the presence of clear  $S_H$ -wave pulses, as indicated by the presence of opposite polarity pulses on each pair of horizontal records. Ideally, the  $S_H$ -wave signals from the 'normal' and 'reverse' source pulses are very nearly inverted images of each other. Digital FFT - IFFT lowpass filtering was used to remove the higher frequency P-wave signal from the  $S_H$ -wave

signal. Different filter cutoffs were used to separate P- and  $S_H$ -waves at different depths, ranging from 600 Hz in the slowest zones to 4000 Hz in the regions of highest velocity. At each depth, the filter frequency was selected to be at least twice the fundamental frequency of the  $S_H$ -wave signal being filtered.

Generally, the first maxima were picked for the 'normal' signals and the first minima for the 'reverse' signals, although other points on the waveform were used if the first pulse was distorted. The absolute arrival time of the 'normal' and 'reverse' signals may vary by +/- 0.2 milliseconds, due to differences in the actuation time of the solenoid source caused by constant mechanical bias in the source or by boring inclination. This variation does not affect the R1-R2 velocity determinations, as the differential time is measured between arrivals of waves created by the same source actuation. The final velocity value is the average of the values obtained from the 'normal' and 'reverse' source actuations.

As with the P-wave data,  $S_H$ -wave velocity calculated from the travel time over the 6.3 foot interval from source to receiver 1 was calculated and plotted for comparison with the velocity derived from the travel time between receivers. In this analysis, the depth values were increased by 4.8 foot to correspond to the mid-point of the 6.3 foot S-R1 interval. Travel times were obtained by picking the first break of the  $S_H$ -wave signal at the near receiver and subtracting 0.3 milliseconds, the calculated and experimentally verified delay from the beginning of the record at the source trigger pulse to source impact.

Independent review of these data and analysis were performed by John Diehl of **GEOVision**.

Figure 3 shows an example of R1 - R2 measurements on a sample filtered suspension record. In Figure 3, the time difference over the 3.3 foot interval of 1.88 milliseconds for the horizontal signals is equivalent to an  $S_H$ -wave velocity of 1745 feet/second. Whenever possible, time differences were determined from several phase points on the  $S_H$ -waveform records to verify the data obtained from the first arrival of the  $S_H$ -wave pulse. Figure 4 displays the same record before filtering of the  $S_H$ -waveform record with a 1400 Hz FFT - IFFT digital lowpass filter,

illustrating the presence of higher frequency P-wave energy at the beginning of the record, and distortion of the lower frequency  $S_H$ -wave by residual P-wave signal.

### **Caliper / Natural Gamma Analysis**

No analysis is required with the caliper or natural gamma data, however depths to identifiable boring features were compared to verify compatible depth readings on all logs. Using WellCAD software version 4.3, these data were combined with the resistivity, ELOG based natural gamma and spontaneous potential (SP) logs, and converted to LAS and PDF formats for transmittal to the client.

### **Resistivity / Natural Gamma / Spontaneous Potential Analysis**

No analysis is required with the resistivity, natural gamma or spontaneous potential data, however depths to identifiable boring features were compared to verify compatible depth readings on all logs. Using WellCAD software version 4.3, these data were combined with the caliper and caliper-based natural gamma logs, and converted to LAS and PDF formats for transmittal to the client.

## Acoustic Televiwer / Boring Deviation Analysis

The collected Acoustic Televiwer data was processed with Robertson Geologging's RGLDIP program, version 6.2, to identify boring features and to extract the deviation data and produce an ASCII file and plots of deviation data.

Sinusoidal projections of both open and hairline fractures in the boring walls were interactively picked on the acoustic reflection image or acoustic travel time image, and are presented on the logs as red sinusoids superimposed over the televiwer images. Bedrock contact, and other bedding planes, when visible, were picked on the same images and are presented on the logs as green sinusoids. The sinusoidal projections were processed to correct for the plunge of the borings using the recorded data from the accelerometers located in the probe, and presented graphically, in what is referred to as "tadpole", or "arrow" format, with true dip indicated by the position of the arrow head on the plot. Direction of dip (not strike) is indicated by the direction of the arrow tail, with true north being "up". These values are presented numerically in columns to the left of the arrow graphic plots. These depth and dip data of the joints and foliation are also presented as .txt files in the boring specific sub-directories on the data disk (CD-R) labeled Report 9333-02 that accompanies this report, and summarized in Table 4.

The televiwer images were processed to create a simulated core image of the borings. It should be considered that the pseudo-core represents a core that would have the full 3.8-inch diameter of the boring, not the 2.5-inch diameter of the cores removed during drilling, so that direct comparison is not possible. Also, the unwrapped image is viewed from the perspective of an observer in the center of the boring looking outward. The simulated core image is viewed from the "outside" of the boring looking inward, so there is a reversal of the position of east and west relative to north between the two images.

## RESULTS

### Suspension Results

Suspension R1-R2 P- and  $S_H$ -wave velocities are plotted in Figures 5 and 8. The suspension velocity data presented in these figures are presented in Tables 5 and 6. The PSLOG and EXCEL analysis files for each boring are included in the boring specific directories on the data disk (CD-R) labeled Report 9333-02 that accompanies this report, along with the raw and filtered waveforms.

P- and  $S_H$ -wave velocity data from R1-R2 and S-R1 analysis, as discussed in the “Suspension Analysis” section of this report, are plotted together in Figures A-1 and A-2 to aid in visual comparison. It must be noted that R1-R2 data is an average velocity over a 3.3 foot segment of the soil column; S-R1 data is an average over 6.3 feet, creating a significant smoothing relative to the R1-R2 plots. S-R1 data are presented in Tables A-1 and A-2, and included in the EXCEL analysis files for each boring on the data disk (CD-R) labeled Report 9333-02 that accompanies this report.

Calibration procedures and records for the suspension measurement system are presented in Appendix D.

The **GEO***Vision* standard field log sheets for all borings are reproduced in Appendix E.

The **GEO***Vision* standard field procedures are reproduced in Appendix F.

## **Caliper/ Natural Gamma Results**

Caliper and natural gamma data are presented in combined log plots with resistivity and spontaneous potential as single page logs in Figures 6 and 9, as well as multi-page logs in Appendix B. LAS 2.0 data and Acrobat files of the plots for each boring are included in the boring specific sub-directories on the data disk (CD-R) labeled Report 9333-02 that accompanies this report.

## **Resistivity / Spontaneous Potential Results**

Resistivity and spontaneous potential data is presented in combined log plots with caliper and natural gamma data as single page logs in Figures 6 and 9, as well as multi-page logs in Appendix B. LAS 2.0 data and Acrobat files of the plots for each boring are included in the boring specific sub-directories on the data disk (CD-R) labeled Report 9333-02 that accompanies this report.

## **Acoustic Televiwer / Boring Deviation Results**

Acoustic televiwer amplitude images and simulated core images are presented in Appendix C, with identified features super-imposed on the images. Features were picked as hairline fractures and bedding planes (as identified as features only present on the amplitude display) and open fractures (as identified as features present on both amplitude and travel-time displays). The same logs are presented in .pdf format in the boring specific sub-directories on the data disk (CD-R) labeled Report 9333-02 that accompanies this report. Fracture and planar feature depth, dip angle and azimuth of dip data are provided numerically on the log sheets, as well as in text format on the data CD-R.

Boring deviation data is presented graphically in Figures 7 and 10, and summarized in Table 4. Deviation data plots in Acrobat format and deviation data at 1.0 foot stations are presented in text format in the boring specific sub-directories of the data disk (CD-R) labeled Report 9333-02 that accompanies this report.

## SUMMARY

### Discussion of Suspension Results

Suspension PS velocity data are ideally collected in an uncased fluid filled boring, drilled with rotary mud (rotary wash) methods. The lower portions of the borings at this site were ideal for collection of suspension PS velocity data.

Suspension PS velocity data quality is judged based upon 5 criteria:

1. Consistent data between receiver to receiver (R1 – R2) and source to receiver (S – R1) data.
2. Consistent relationship between P-wave and  $S_H$  -wave (excluding transition to saturated soils)
3. Consistency between data from adjacent depth intervals.
4. Clarity of P-wave and  $S_H$ -wave onset, as well as damping of later oscillations.
5. Consistency of profile between adjacent borings, if available.

M-10DH: These data show excellent correlation between R1 – R2 and S – R1 data, as well as excellent correlation between P-wave and  $S_H$ -wave velocities.  $S_H$ -wave onsets are generally clear, and later oscillations are well damped. P-wave arrivals are weak, as is generally the case in hard rock borings, and above water table in soil. In the hard rock, low velocity regions correspond well with fracture zones identified on the acoustic televiewer logs. This is an excellent rock velocity data set, with good soil velocity data.

M-30DH: These data show excellent correlation between R1 – R2 and S – R1 data, as well as excellent correlation between P-wave and  $S_H$ -wave velocities.  $S_H$ -wave onsets are generally clear, and later oscillations are well damped. P-wave arrivals are weak, as is generally the case in hard rock borings, and above water table in soil. In the hard rock, low velocity regions correspond well with fracture zones identified on the acoustic televiewer logs. This is an excellent rock velocity data set, with good soil velocity data.

## **Discussion of Caliper / Natural Gamma Results**

Caliper and natural gamma data was collected for the entire depth of each boring. The caliper logs for all these borings show very consistent gauge in competent rock, with minor tapering downhole due to bit wear. Some fracturing is noted, but below the rock contact, the borings are generally tight. Natural gamma was collected with this tool in all the borings, as well as with the ELOG probe, and the comparison between the two data sets provides an almost exact match, verifying the performance of the natural gamma measuring systems.

## **Discussion of Resistivity / Spontaneous Potential Results**

Both long and short normal resistivity and single point resistance provide clear delineation of different lithologic units and changes within the bedrock, showing drops in resistivity at weathered zones that correspond with changes in natural gamma and velocity data. The electrical data is not valid above 40 feet, as the upper yoke electrode moves out of the boring fluid at this depth. The natural gamma data agrees well with the natural gamma data collected with the caliper probe. The comparison between the two data sets provides an almost exact match, verifying the performance of the natural gamma measuring systems.

## **Discussion of Acoustic Televiewer / Boring Deviation Results**

The acoustic televiewer data quality in the rock section of both borings is very good, providing clear images of a number of fractures and beading planes. Many of the borings exhibit diagonal banding (zebra striping) caused by rapid reaming down the boring with new core bits that are slightly larger than the gauge of the original boring. This creates a spiral wear pattern in the boring that alters the characteristic smooth surface of diamond cored borings. This wear pattern can have a significant impact on acoustic televiewer image quality, and in these borings may conceal smaller features. It will not conceal fractures, however.

Location of fractures and weathered zones on the televiewer logs correspond precisely with increases in caliper log diameter and suspension PS velocity drops.

The borings were inclined at 3.9 degrees, or less, from vertical, and the maximum error in depth value was 0.5 feet in 200 ft, or less than 0.3 percent, as presented in Table 4. This error is less than depth errors from other causes, and no adjustment of log depth is indicated.

## **Quality Assurance**

These boring geophysical measurements were performed using industry-standard or better methods for measurements and analyses. All work was performed under **GEOVision** data collection and processing procedures, which include:

- Use of NIST-traceable calibrations, where applicable, for field and laboratory instrumentation
- Use of standard field data logs
- Use of independent verification of velocity data by comparison of receiver-to-receiver and source-to-receiver velocities
- Independent review of calculations and results by a registered professional engineer, geologist, or geophysicist.

## **Suspension Data Reliability**

P- and  $S_H$ -wave velocity measurement using the Suspension Method gives average velocities over a 3.3 foot interval of depth. This high resolution results in the scatter of values shown in the graphs. Individual measurements are very reliable with estimated precision of +/- 5%. Standardized field procedures and comparison checks contribute to the reliability of these data.

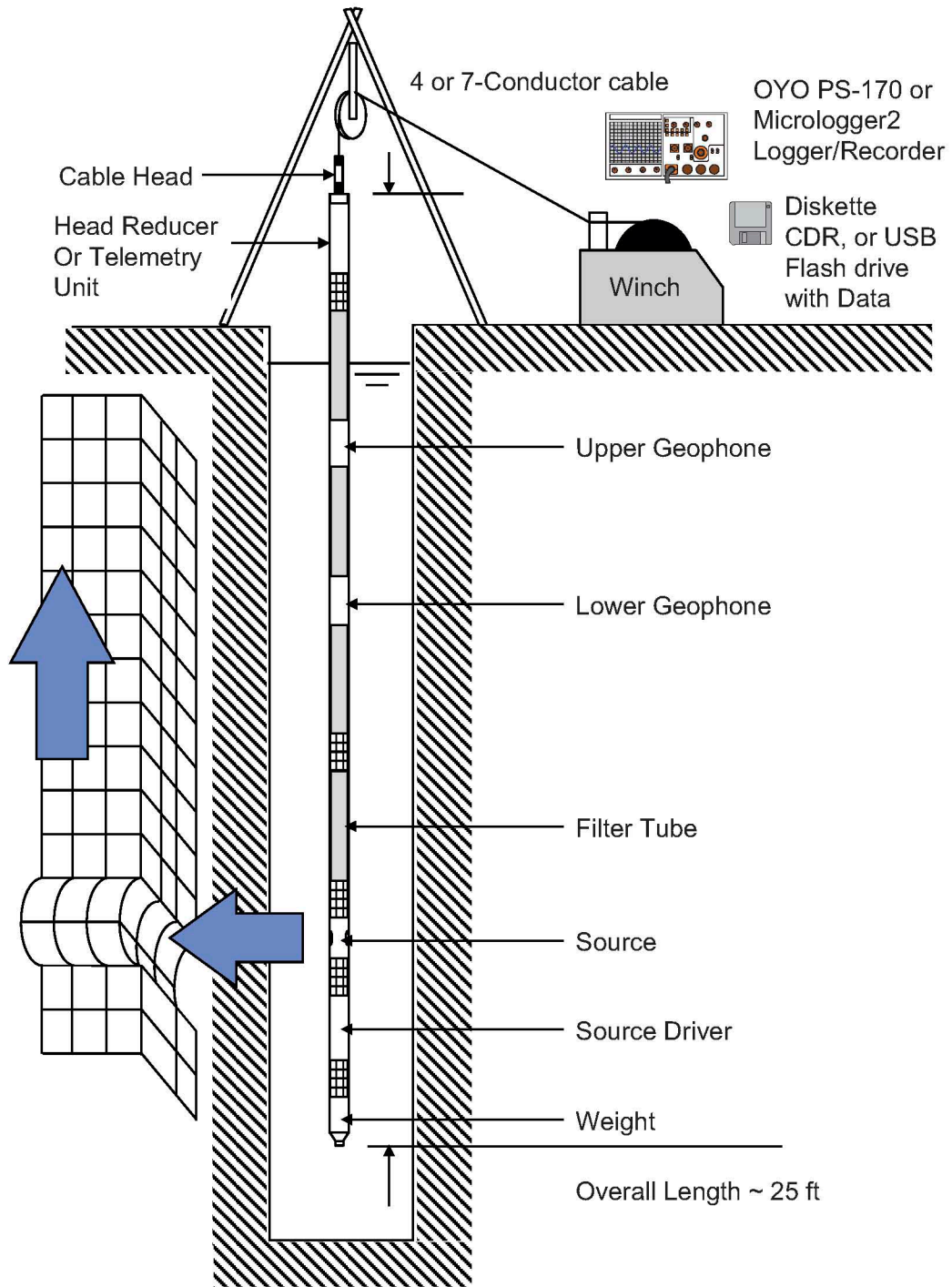


Figure 1: Concept illustration of P-S logging system

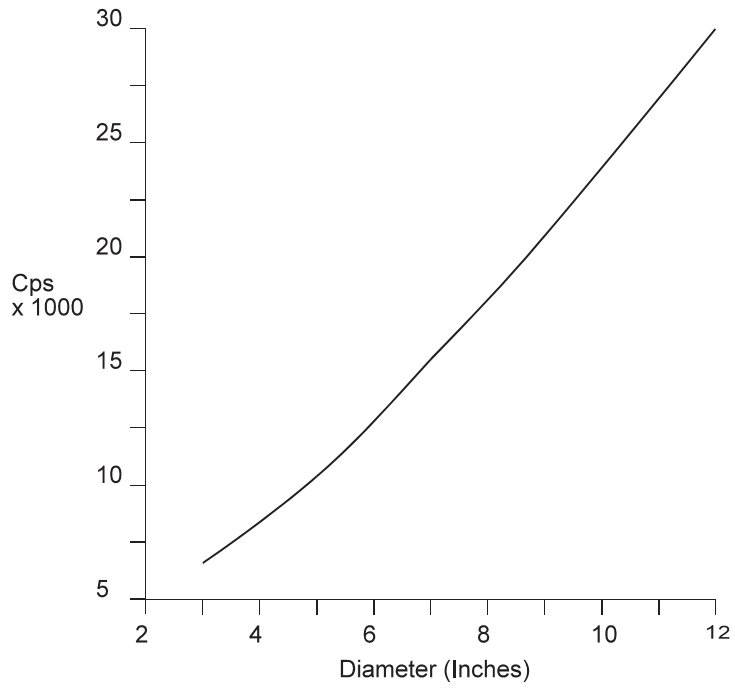


Figure 2. Example Calibration Curve for Caliper Probe

BORING DESIGNATION	DATES LOGGED	ELEVATION*	COORDINATES* - FEET	
			NORTH (Y)	EAST (X)
M-10DH	9/16-17/2009	323.61	3909243.32	11685945.83
M-30DH	9/15-17/2009	313.34	3909694.92	11685381.66

\* All points referenced to Control Monument 7 and adjusted to reflect the following Datums  
 Horizontal – VSPCS South Zone, NAD 83(CORS96)(EPOCH:2002)  
 Elevation - NAVD88 (Geoid03)  
 Survey data provided by MACTEC

Table 1 Boring locations and logging dates

BORING NUMBER	TOOL AND RUN NUMBER	DEPTH RANGE (FEET)	OPEN HOLE (FEET)	DEPTH TO BOTTOM OF CASING (FEET)	SAMPLE INTERVAL (FEET)	DATE LOGGED
M-10DH	ELOG/GAMMA 1	200.1 – 86.0	200.1	89.8 STEEL	0.05	9/16/2009
M-10DH	SUSPENSION 1	91.9 – 187.0	-	89.8 STEEL	1.6	9/16/2009
M-10DH	ACOUSTIC TELEVIEWER 1	196.9 - 86.9	-	89.8 STEEL	0.008	9/16/2009
M-10DH	CALIPER/GAMMA 1	198.8 - 84.0	-	89.8 STEEL	0.05	9/16/2009
M-10DH	ELOG/GAMMA 2	105.6 – 36.6	-	7.0 STEEL	0.05	9/16/2009
M-10DH	SUSPENSION 2	8.2 – 98.4	-	7.0 STEEL	1.6	9/17/2009
M-10DH	CALIPER/GAMMA 2	100.9 – 3.9	-	7.0 STEEL	0.05	9/17/2009
M-10DH	ACOUSTIC TELEVIEWER 2	99.4 – 2.8	-	7.0 STEEL	0.008	9/18/2009
M-30DH	ELOG/GAMMA 1	200.5 – 39.6	200.5	44.0 STEEL	0.05	9/15/2009
M-30DH	ELOG/GAMMA 2	75.0 – 39.9	-	44.0 STEEL	0.05	9/15/2009
M-30DH	SUSPENSION 1	45.9 – 187.0	-	44.0 STEEL	1.6	9/15/2009
M-30DH	ACOUSTIC TELEVIEWER 1	200.2 – 40.2	-	44.0 STEEL	0.008	9/16/2009
M-30DH	ACOUSTIC TELEVIEWER 2	55.4 – 41.8	-	44.0 STEEL	0.008	9/16/2009
M-30DH	CALIPER/GAMMA 1	200.1 – 33.2	-	44.0 STEEL	0.05	9/16/2009
M-30DH	ELOG/GAMMA 3	65.4 – 34.3	-	7.0 STEEL	0.05	9/17/2009
M-30DH	SUSPENSION 2	8.2 – 52.5	-	7.0 STEEL	1.6	9/17/2009
M-30DH	ACOUSTIC TELEVIEWER 3	45.9 – 5.9	-	7.0 STEEL	0.008	9/17/2009
M-30DH	CALIPER/GAMMA 2	50.7 – 3.3	-	7.0 STEEL	0.05	9/17/2009

- PROBE DID NOT TOUCH BOTTOM OF BORING

Table 2. Logging dates and depth ranges

BORING NUMBER	TOOL AND RUN NUMBER	TOOL HIT BOTTOM DEPTH (FEET)	DRILLER DEPTH (FEET)	STARTING DEPTH REF. (FEET)	ENDING DEPTH REF. (FEET)	ASDE (FEET)
M-10DH	ELOG/GAMMA 1	201.1	201.9	39.5	39.5	0
M-10DH	SUSPENSION 1	-		6.7	6.7	0
M-10DH	ACOUSTIC TELEVIEWER 1	-		3.2	3.2	0
M-10DH	CALIPER/GAMMA 1	-		5.3	5.3	0
M-10DH	ELOG/GAMMA 2	-		32.2	32.2	0
M-10DH	SUSPENSION 2	-		5.4	5.4	0
M-10DH	CALIPER/GAMMA 2	-		4.0	4.0	0
M-10DH	ACOUSTIC TELEVIEWER 2	-		2.8	2.7	0.1
M-30DH	ELOG/GAMMA 1	200.5	201.7	39.9	39.6	0.3
M-30DH	ELOG/GAMMA 2	-		39.9	40.0	0.1
M-30DH	SUSPENSION 1	-		7.1	7.1	0
M-30DH	ACOUSTIC TELEVIEWER 1	-		3.6	3.6	0
M-30DH	ACOUSTIC TELEVIEWER 2	-		3.6	3.6	0
M-30DH	CALIPER/GAMMA 1	-		5.7	5.7	0
M-30DH	ELOG/GAMMA 3	-		37.7	37.8	0.1
M-30DH	SUSPENSION 2	-		4.9	4.9	0
M-30DH	ACOUSTIC TELEVIEWER 3	-		1.4	1.4	0
M-30DH	CALIPER/GAMMA 2	-		3.5	3.5	0

- PROBE DID NOT TOUCH BOTTOM OF BORING

Table 3. Boring Bottom Depths and After Survey Depth Error (ASDE)

BORING NUMBER	MEAN DEVIATION AND AZIMUTH (DEGREES)	SURVEY DEPTH (FEET)	VERTICAL DEPTH (FEET)	DEPTH ERROR (FEET)	HORIZONTAL OFFSET (FEET)
M-10DH	3.9 – N328	196.9	196.4	0.5	13.3
M-30DH	1.6 – N159	200.2	200.2	0	5.5

Table 4. Boring Deviation Data Summary

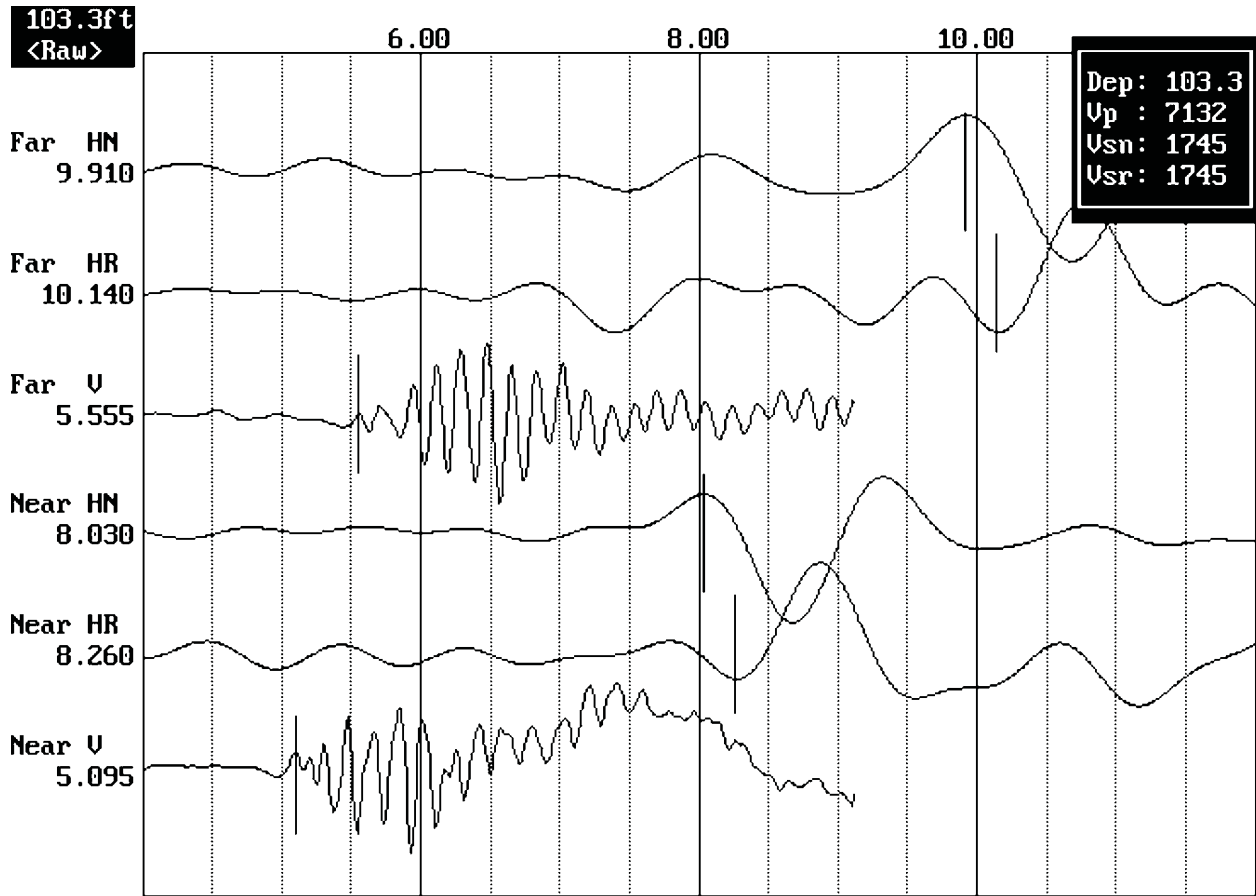


Figure 3: Example of filtered (1400 Hz lowpass) record

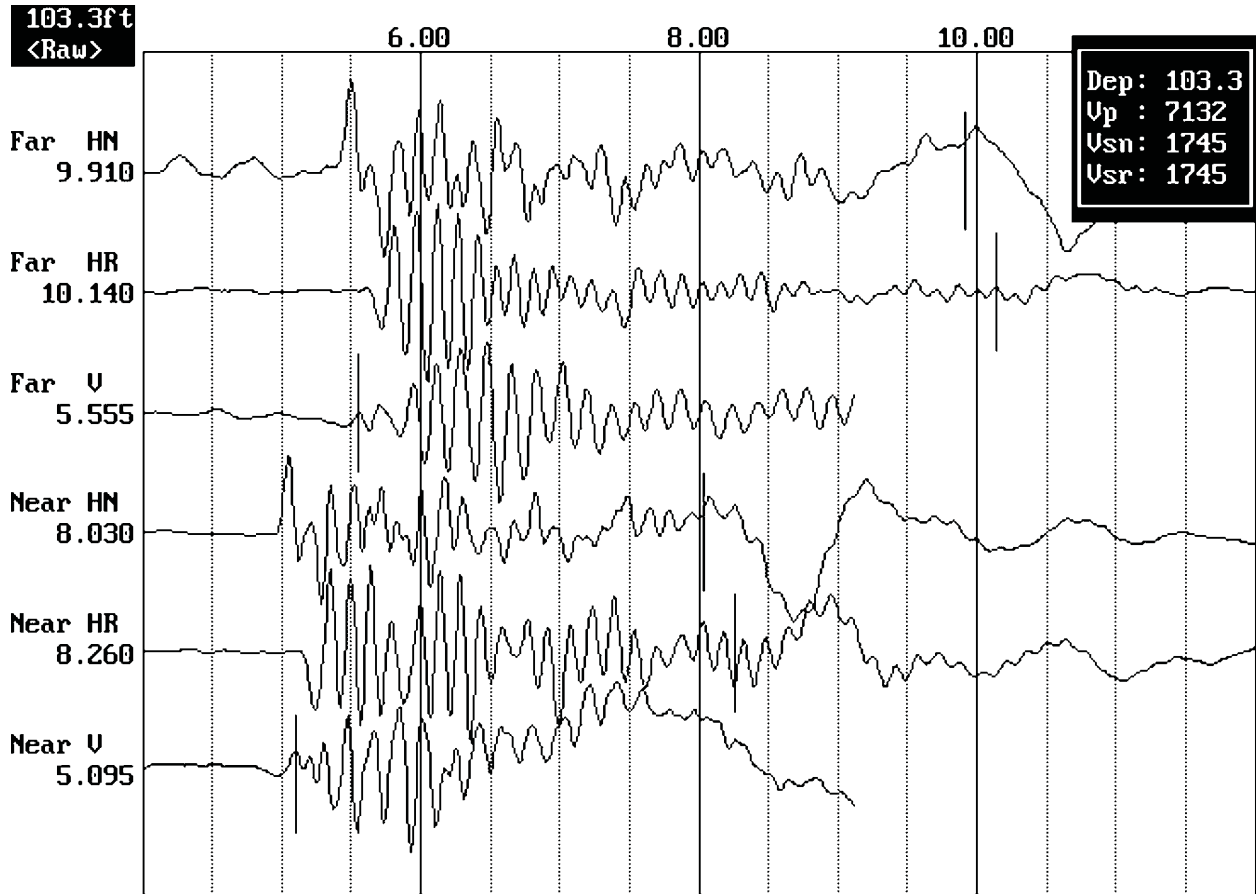


Figure 4. Example of unfiltered record

### NORTH ANNA BORING M-10DH Receiver to Receiver $V_s$ and $V_p$ Analysis

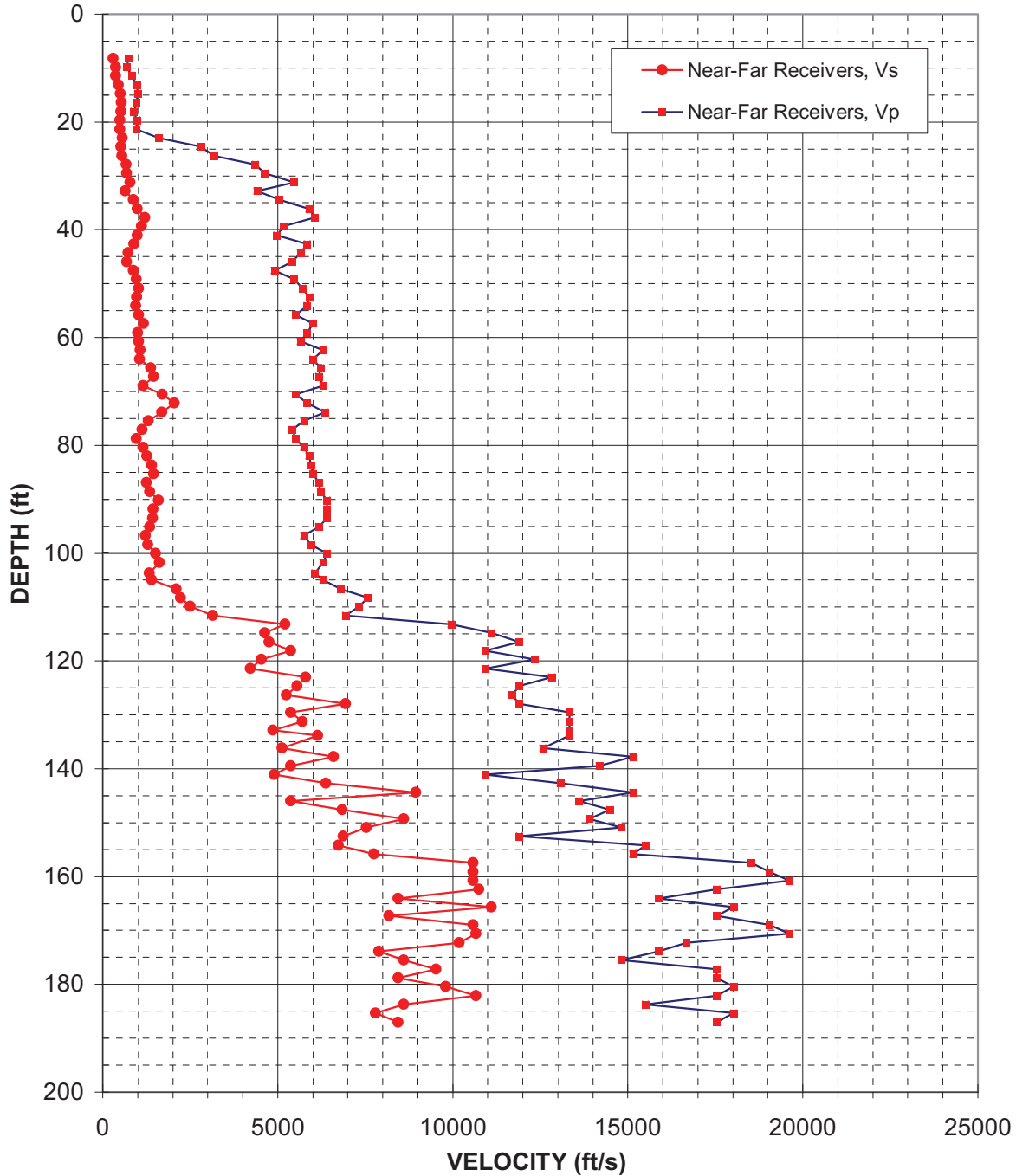


Figure 5: Boring M-10DH, Suspension R1-R2 P- and  $S_H$ -wave velocities

Table 5. Boring M-10DH, Suspension R1-R2 depths and P- and S<sub>H</sub>-wave velocities

**Summary of Compressional Wave Velocity, Shear Wave Velocity, and Poisson's Ratio  
 Based on Receiver-to-Receiver Travel Time Data - Borehole M-10DH**

American Units				Metric Units			
Depth at Midpoint Between Receivers	Velocity		Poisson's Ratio	Depth at Midpoint Between Receivers	Velocity		Poisson's Ratio
	V <sub>s</sub>	V <sub>p</sub>			V <sub>s</sub>	V <sub>p</sub>	
(ft)	(ft/s)	(ft/s)		(m)	(m/s)	(m/s)	
8.2	300	740	0.40	2.5	90	230	0.40
9.8	370	690	0.29	3.0	110	210	0.29
11.5	370	840	0.38	3.5	110	250	0.38
13.1	460	970	0.36	4.0	140	300	0.36
14.8	510	1010	0.33	4.5	160	310	0.33
16.4	530	960	0.28	5.0	160	290	0.28
18.0	520	890	0.24	5.5	160	270	0.24
19.7	500	980	0.32	6.0	150	300	0.32
21.3	490	960	0.32	6.5	150	290	0.32
23.0	560	1610	0.43	7.0	170	490	0.43
24.6	520	2800	0.48	7.5	160	850	0.48
26.3	550	3170	0.48	8.0	170	970	0.48
27.9	670	4360	0.49	8.5	200	1330	0.49
29.5	690	4630	0.49	9.0	210	1410	0.49
31.2	790	5460	0.49	9.5	240	1670	0.49
32.8	650	4420	0.49	10.0	200	1350	0.49
34.5	880	5050	0.48	10.5	270	1540	0.48
36.1	1000	5900	0.49	11.0	300	1800	0.49
37.7	1210	6060	0.48	11.5	370	1850	0.48
39.4	1110	5170	0.48	12.0	340	1580	0.48
41.0	1000	4980	0.48	12.5	300	1520	0.48
42.7	890	5850	0.49	13.0	270	1780	0.49
44.3	730	5650	0.49	13.5	220	1720	0.49
45.9	690	5420	0.49	14.0	210	1650	0.49
47.6	880	4900	0.48	14.5	270	1490	0.48
49.2	970	5460	0.48	15.0	290	1670	0.48
50.9	1030	5700	0.48	15.5	310	1740	0.48
52.5	980	5900	0.49	16.0	300	1800	0.49
54.1	960	5850	0.49	16.5	290	1780	0.49
55.8	1030	5510	0.48	17.0	310	1680	0.48
57.4	1170	6010	0.48	17.5	360	1830	0.48
59.1	1000	5850	0.49	18.0	300	1780	0.49
60.7	1030	5650	0.48	18.5	310	1720	0.48
62.3	1070	6290	0.49	19.0	330	1920	0.49
64.0	1060	6010	0.48	19.5	320	1830	0.48
65.6	1370	6230	0.47	20.0	420	1900	0.47

**Summary of Compressional Wave Velocity, Shear Wave Velocity, and Poisson's Ratio  
 Based on Receiver-to-Receiver Travel Time Data - Borehole M-10DH**

American Units			
Depth at Midpoint Between Receivers	Velocity		Poisson's Ratio
	V <sub>s</sub>	V <sub>p</sub>	
(ft)	(ft/s)	(ft/s)	
67.3	1460	6170	0.47
68.9	1150	6290	0.48
70.5	1710	5510	0.45
72.2	2040	5850	0.43
73.8	1690	6350	0.46
75.5	1310	5750	0.47
77.1	1130	5420	0.48
78.7	970	5510	0.48
80.4	1150	5750	0.48
82.0	1260	5900	0.48
83.7	1410	5950	0.47
85.3	1460	6010	0.47
86.9	1250	6170	0.48
88.6	1340	6230	0.48
90.2	1590	6410	0.47
91.9	1450	6410	0.47
93.5	1420	6410	0.47
95.1	1350	6170	0.47
96.8	1230	5750	0.48
98.4	1290	5950	0.48
100.1	1520	6410	0.47
101.7	1620	6290	0.46
103.7	1340	6060	0.47
105.0	1400	6290	0.47
106.6	2100	6800	0.45
108.3	2220	7580	0.45
109.9	2500	7330	0.43
111.6	3140	6940	0.37
113.2	5210	9950	0.31
114.8	4630	11110	0.39
116.5	4760	11900	0.40
118.1	5380	10930	0.34
119.8	4540	12350	0.42
121.4	4220	10930	0.41
123.0	5800	12820	0.37
124.7	5560	11900	0.36
126.3	5250	11700	0.37
128.0	6940	11900	0.24
129.6	5380	13330	0.40

Metric Units			
Depth at Midpoint Between Receivers	Velocity		Poisson's Ratio
	V <sub>s</sub>	V <sub>p</sub>	
(m)	(m/s)	(m/s)	
20.5	450	1880	0.47
21.0	350	1920	0.48
21.5	520	1680	0.45
22.0	620	1780	0.43
22.5	520	1940	0.46
23.0	400	1750	0.47
23.5	340	1650	0.48
24.0	290	1680	0.48
24.5	350	1750	0.48
25.0	380	1800	0.48
25.5	430	1810	0.47
26.0	440	1830	0.47
26.5	380	1880	0.48
27.0	410	1900	0.48
27.5	490	1950	0.47
28.0	440	1950	0.47
28.5	430	1950	0.47
29.0	410	1880	0.47
29.5	370	1750	0.48
30.0	390	1810	0.48
30.5	460	1950	0.47
31.0	490	1920	0.46
31.6	410	1850	0.47
32.0	430	1920	0.47
32.5	640	2070	0.45
33.0	680	2310	0.45
33.5	760	2230	0.43
34.0	960	2120	0.37
34.5	1590	3030	0.31
35.0	1410	3390	0.39
35.5	1450	3630	0.40
36.0	1640	3330	0.34
36.5	1380	3760	0.42
37.0	1290	3330	0.41
37.5	1770	3910	0.37
38.0	1690	3630	0.36
38.5	1600	3560	0.37
39.0	2120	3630	0.24
39.5	1640	4060	0.40

**Summary of Compressional Wave Velocity, Shear Wave Velocity, and Poisson's Ratio  
 Based on Receiver-to-Receiver Travel Time Data - Borehole M-10DH**

American Units			
Depth at Midpoint Between Receivers	Velocity		Poisson's Ratio
	V <sub>s</sub>	V <sub>p</sub>	
(ft)	(ft/s)	(ft/s)	
131.2	5700	13330	0.39
132.9	4870	13330	0.42
133.9	6140	13330	0.37
136.2	5130	12580	0.40
137.8	6600	15150	0.38
139.4	5380	14180	0.42
141.1	4900	10930	0.37
142.7	6380	13070	0.34
144.4	8950	15150	0.23
146.0	5380	13610	0.41
147.6	6840	14490	0.36
149.3	8600	13890	0.19
150.9	7530	14810	0.33
152.6	6870	11900	0.25
154.2	6730	15500	0.38
155.8	7750	15150	0.32
157.5	10580	18520	0.26
159.1	10580	19050	0.28
160.8	10580	19610	0.29
162.4	10750	17540	0.20
164.0	8440	15870	0.30
165.7	11110	18020	0.19
167.3	8180	17540	0.36
169.0	10580	19050	0.28
170.6	10670	19610	0.29
172.2	10180	16670	0.20
173.9	7890	15870	0.34
175.5	8600	14810	0.25
177.2	9520	17540	0.29
178.8	8440	17540	0.35
180.5	9800	18020	0.29
182.1	10670	17540	0.21
183.7	8600	15500	0.28
185.4	7800	18020	0.38
187.0	8440	17540	0.35

Metric Units			
Depth at Midpoint Between Receivers	Velocity		Poisson's Ratio
	V <sub>s</sub>	V <sub>p</sub>	
(m)	(m/s)	(m/s)	
40.0	1740	4060	0.39
40.5	1480	4060	0.42
40.8	1870	4060	0.37
41.5	1560	3830	0.40
42.0	2010	4620	0.38
42.5	1640	4320	0.42
43.0	1490	3330	0.37
43.5	1940	3980	0.34
44.0	2730	4620	0.23
44.5	1640	4150	0.41
45.0	2080	4420	0.36
45.5	2620	4230	0.19
46.0	2300	4520	0.33
46.5	2090	3630	0.25
47.0	2050	4730	0.38
47.5	2360	4620	0.32
48.0	3230	5640	0.26
48.5	3230	5810	0.28
49.0	3230	5980	0.29
49.5	3280	5350	0.20
50.0	2570	4840	0.30
50.5	3390	5490	0.19
51.0	2490	5350	0.36
51.5	3230	5810	0.28
52.0	3250	5980	0.29
52.5	3100	5080	0.20
53.0	2400	4840	0.34
53.5	2620	4520	0.25
54.0	2900	5350	0.29
54.5	2570	5350	0.35
55.0	2990	5490	0.29
55.5	3250	5350	0.21
56.0	2620	4730	0.28
56.5	2380	5490	0.38
57.0	2570	5350	0.35

**Notes:**        "-" means no data available at that particular interval of depth.

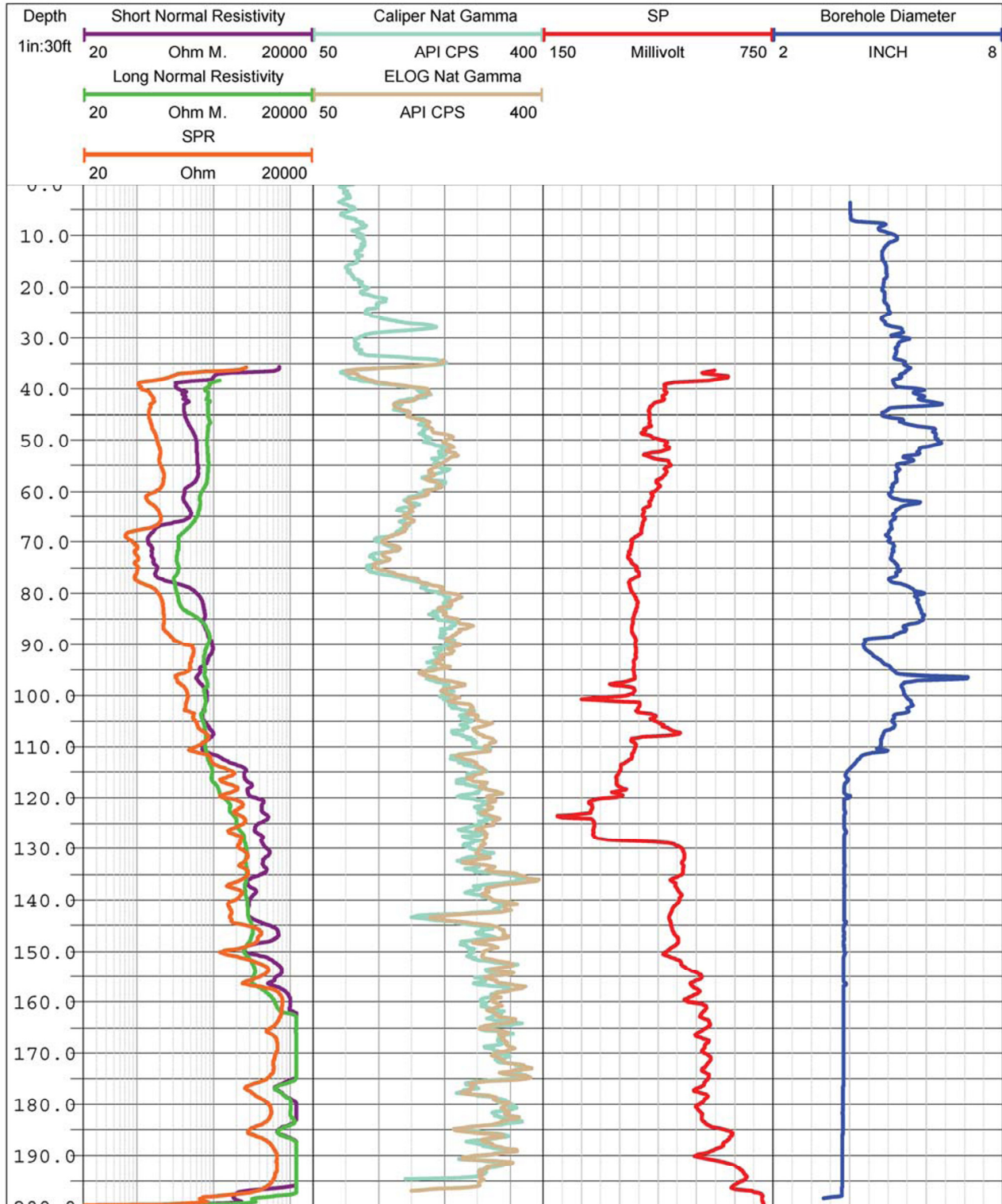


Figure 6: Boring M-10DH, Caliper, Natural gamma, Resistivity and SP logs

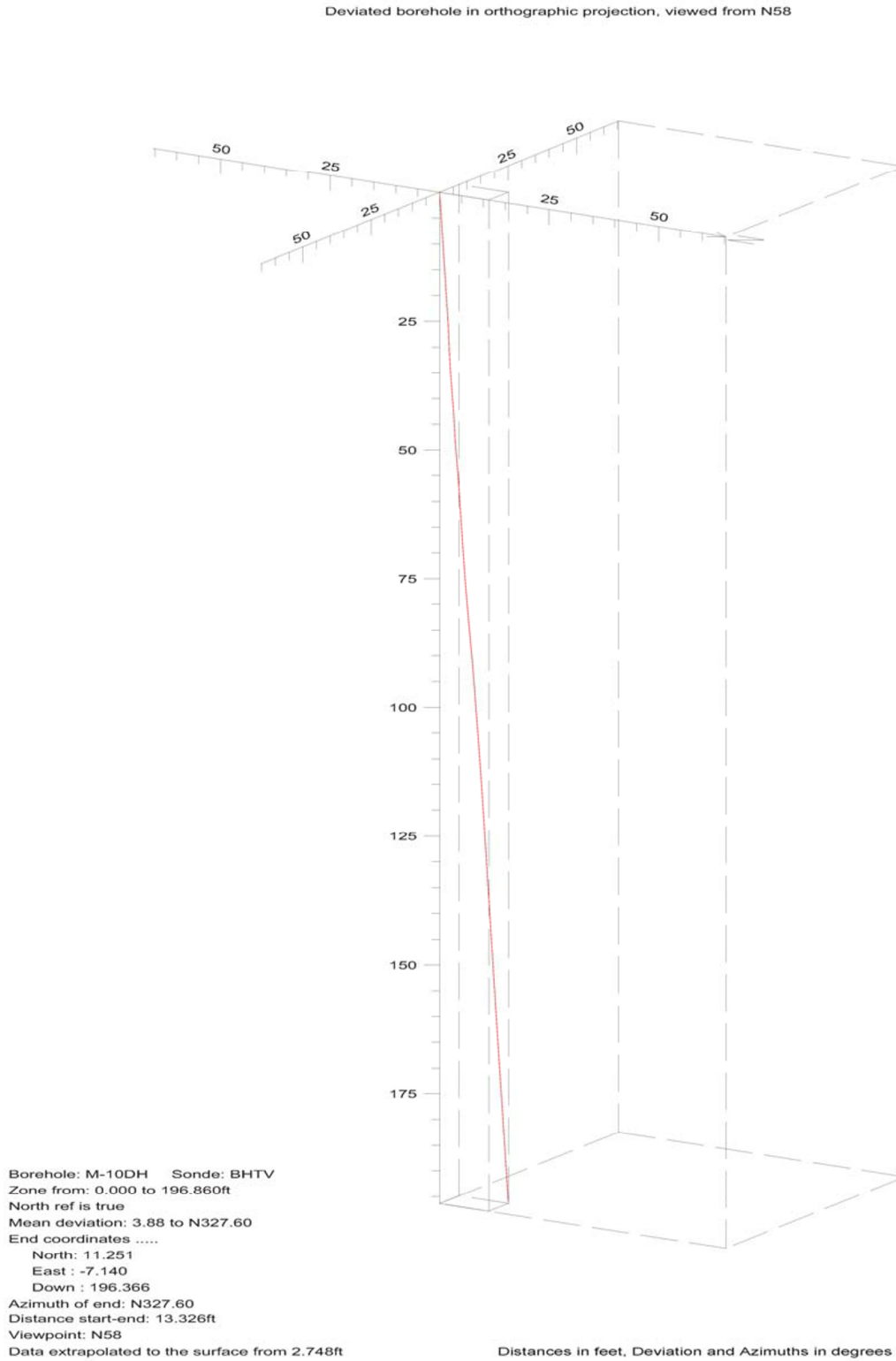


Figure 7. Boring M-10DH, Deviation Projection

### NORTH ANNA BORING M-30DH Receiver to Receiver $V_s$ and $V_p$ Analysis

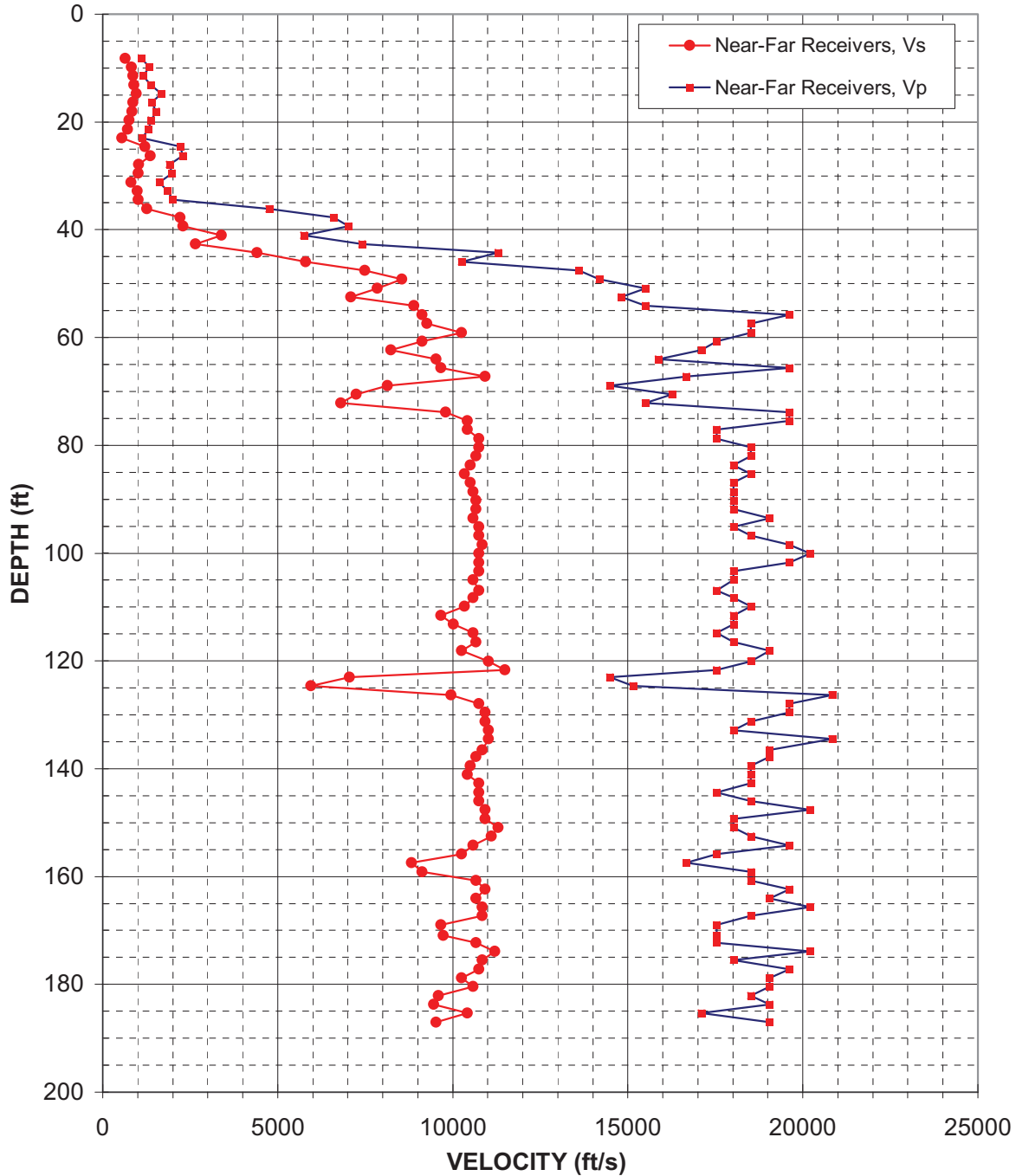


Figure 8: Boring M-30DH, Suspension R1-R2 P- and  $S_H$ -wave velocities

Table 6. Boring M-30DH, Suspension R1-R2 depths and P- and S<sub>H</sub>-wave velocities

**Summary of Compressional Wave Velocity, Shear Wave Velocity, and Poisson's Ratio  
 Based on Receiver-to-Receiver Travel Time Data - Borehole M-30DH**

American Units				Metric Units			
Depth at Midpoint Between Receivers	Velocity		Poisson's Ratio	Depth at Midpoint Between Receivers	Velocity		Poisson's Ratio
	V <sub>s</sub>	V <sub>p</sub>			V <sub>s</sub>	V <sub>p</sub>	
(ft)	(ft/s)	(ft/s)		(m)	(m/s)	(m/s)	
8.2	650	1110	0.24	2.5	200	340	0.24
9.8	830	1330	0.18	3.0	250	400	0.18
11.5	870	1160	-	3.5	260	350	-
13.1	890	1380	0.13	4.0	270	420	0.13
14.8	960	1680	0.26	4.5	290	510	0.26
16.4	870	1410	0.19	5.0	260	430	0.19
18.0	840	1530	0.29	5.5	260	470	0.29
19.7	760	1390	0.29	6.0	230	420	0.29
21.3	710	1310	0.29	6.5	220	400	0.29
23.0	560	1130	0.34	7.0	170	340	0.34
24.6	1200	2220	0.29	7.5	370	680	0.29
26.3	1370	2280	0.22	8.0	420	700	0.22
27.9	1030	1900	0.29	8.5	310	580	0.29
29.5	1020	1980	0.32	9.0	310	600	0.32
31.2	810	1630	0.34	9.5	250	500	0.34
32.8	990	1850	0.30	10.0	300	560	0.30
34.5	1020	2010	0.33	10.5	310	610	0.33
36.1	1270	4760	0.46	11.0	390	1450	0.46
37.7	2210	6600	0.44	11.5	670	2010	0.44
39.4	2300	7020	0.44	12.0	700	2140	0.44
41.0	3400	5750	0.23	12.5	1040	1750	0.23
42.7	2660	7410	0.43	13.0	810	2260	0.43
44.3	4420	11300	0.41	13.5	1350	3440	0.41
45.9	5800	10260	0.27	14.0	1770	3130	0.27
47.6	7490	13610	0.28	14.5	2280	4150	0.28
49.2	8550	14180	0.21	15.0	2610	4320	0.21
50.9	7840	15500	0.33	15.5	2390	4730	0.33
52.5	7090	14810	0.35	16.0	2160	4520	0.35
54.1	8890	15500	0.26	16.5	2710	4730	0.26
55.8	9130	19610	0.36	17.0	2780	5980	0.36
57.4	9260	18520	0.33	17.5	2820	5640	0.33
59.1	10260	18520	0.28	18.0	3130	5640	0.28
60.7	9130	17540	0.31	18.5	2780	5350	0.31
62.3	8230	17090	0.35	19.0	2510	5210	0.35
64.0	9520	15870	0.22	19.5	2900	4840	0.22
65.6	9660	19610	0.34	20.0	2940	5980	0.34
67.3	10930	16670	0.12	20.5	3330	5080	0.12

**Summary of Compressional Wave Velocity, Shear Wave Velocity, and Poisson's Ratio  
 Based on Receiver-to-Receiver Travel Time Data - Borehole M-30DH**

American Units			
Depth at Midpoint Between Receivers	Velocity		Poisson's Ratio
	V <sub>s</sub>	V <sub>p</sub>	
(ft)	(ft/s)	(ft/s)	
68.9	8130	14490	0.27
70.5	7250	16260	0.38
72.2	6800	15500	0.38
73.8	9800	19610	0.33
75.5	10420	19610	0.30
77.1	10420	17540	0.23
78.7	10750	17540	0.20
80.4	10750	18520	0.25
82.0	10670	18520	0.25
83.7	10500	18020	0.24
85.3	10340	18520	0.27
86.9	10500	18020	0.24
88.6	10580	18020	0.24
90.2	10670	18020	0.23
91.9	10670	18020	0.23
93.5	10580	19050	0.28
95.1	10750	18020	0.22
96.8	10750	18520	0.25
98.4	10840	19610	0.28
100.1	10750	20200	0.30
101.7	10750	19610	0.28
103.4	10750	18020	0.22
105.0	10580	18020	0.24
107.0	10750	17540	0.20
108.3	10580	18020	0.24
109.9	10340	18520	0.27
111.6	9660	18020	0.30
113.2	10030	18020	0.28
114.8	10580	17540	0.21
116.5	10670	18020	0.23
118.1	10260	19050	0.30
120.1	11020	18520	0.23
121.7	11490	17540	0.12
123.0	7050	14490	0.34
124.7	5950	15150	0.41
126.3	9950	20830	0.35
128.0	10750	19610	0.28
129.6	10930	19610	0.27
131.2	10930	18520	0.23

Metric Units			
Depth at Midpoint Between Receivers	Velocity		Poisson's Ratio
	V <sub>s</sub>	V <sub>p</sub>	
(m)	(m/s)	(m/s)	
21.0	2480	4420	0.27
21.5	2210	4960	0.38
22.0	2070	4730	0.38
22.5	2990	5980	0.33
23.0	3180	5980	0.30
23.5	3180	5350	0.23
24.0	3280	5350	0.20
24.5	3280	5640	0.25
25.0	3250	5640	0.25
25.5	3200	5490	0.24
26.0	3150	5640	0.27
26.5	3200	5490	0.24
27.0	3230	5490	0.24
27.5	3250	5490	0.23
28.0	3250	5490	0.23
28.5	3230	5810	0.28
29.0	3280	5490	0.22
29.5	3280	5640	0.25
30.0	3300	5980	0.28
30.5	3280	6160	0.30
31.0	3280	5980	0.28
31.5	3280	5490	0.22
32.0	3230	5490	0.24
32.6	3280	5350	0.20
33.0	3230	5490	0.24
33.5	3150	5640	0.27
34.0	2940	5490	0.30
34.5	3060	5490	0.28
35.0	3230	5350	0.21
35.5	3250	5490	0.23
36.0	3130	5810	0.30
36.6	3360	5640	0.23
37.1	3500	5350	0.12
37.5	2150	4420	0.34
38.0	1810	4620	0.41
38.5	3030	6350	0.35
39.0	3280	5980	0.28
39.5	3330	5980	0.27
40.0	3330	5640	0.23

**Summary of Compressional Wave Velocity, Shear Wave Velocity, and Poisson's Ratio  
Based on Receiver-to-Receiver Travel Time Data - Borehole M-30DH**

American Units			
Depth at Midpoint Between Receivers	Velocity		Poisson's Ratio
	V <sub>s</sub>	V <sub>p</sub>	
(ft)	(ft/s)	(ft/s)	
132.9	11020	18020	0.20
134.5	11020	20830	0.31
136.5	10840	19050	0.26
137.8	10670	19050	0.27
139.4	10500	18520	0.26
141.1	10420	18520	0.27
142.7	10750	18520	0.25
144.4	10750	17540	0.20
146.0	10750	18520	0.25
147.6	10930	20200	0.29
149.3	10930	18020	0.21
150.9	11300	18020	0.18
152.6	11110	18520	0.22
154.2	10580	19610	0.29
155.8	10260	17540	0.24
157.5	8830	16670	0.30
159.1	9130	18520	0.34
160.8	10670	18520	0.25
162.4	10930	19610	0.27
164.0	10670	19050	0.27
165.7	10840	20200	0.30
167.3	10840	18520	0.24
169.0	9660	17540	0.28
170.9	9730	17540	0.28
172.2	10670	17540	0.21
173.9	11200	20200	0.28
175.5	10840	18020	0.22
177.2	10750	19610	0.28
178.8	10260	19050	0.30
180.5	10580	19050	0.28
182.1	9590	18520	0.32
183.7	9460	19050	0.34
185.4	10420	17090	0.20
187.0	9520	19050	0.33

Metric Units			
Depth at Midpoint Between Receivers	Velocity		Poisson's Ratio
	V <sub>s</sub>	V <sub>p</sub>	
(m)	(m/s)	(m/s)	
40.5	3360	5490	0.20
41.0	3360	6350	0.31
41.6	3300	5810	0.26
42.0	3250	5810	0.27
42.5	3200	5640	0.26
43.0	3180	5640	0.27
43.5	3280	5640	0.25
44.0	3280	5350	0.20
44.5	3280	5640	0.25
45.0	3330	6160	0.29
45.5	3330	5490	0.21
46.0	3440	5490	0.18
46.5	3390	5640	0.22
47.0	3230	5980	0.29
47.5	3130	5350	0.24
48.0	2690	5080	0.30
48.5	2780	5640	0.34
49.0	3250	5640	0.25
49.5	3330	5980	0.27
50.0	3250	5810	0.27
50.5	3300	6160	0.30
51.0	3300	5640	0.24
51.5	2940	5350	0.28
52.1	2970	5350	0.28
52.5	3250	5350	0.21
53.0	3420	6160	0.28
53.5	3300	5490	0.22
54.0	3280	5980	0.28
54.5	3130	5810	0.30
55.0	3230	5810	0.28
55.5	2920	5640	0.32
56.0	2880	5810	0.34
56.5	3180	5210	0.20
57.0	2900	5810	0.33

**Notes:**        "-" means no data available at that particular interval of depth.

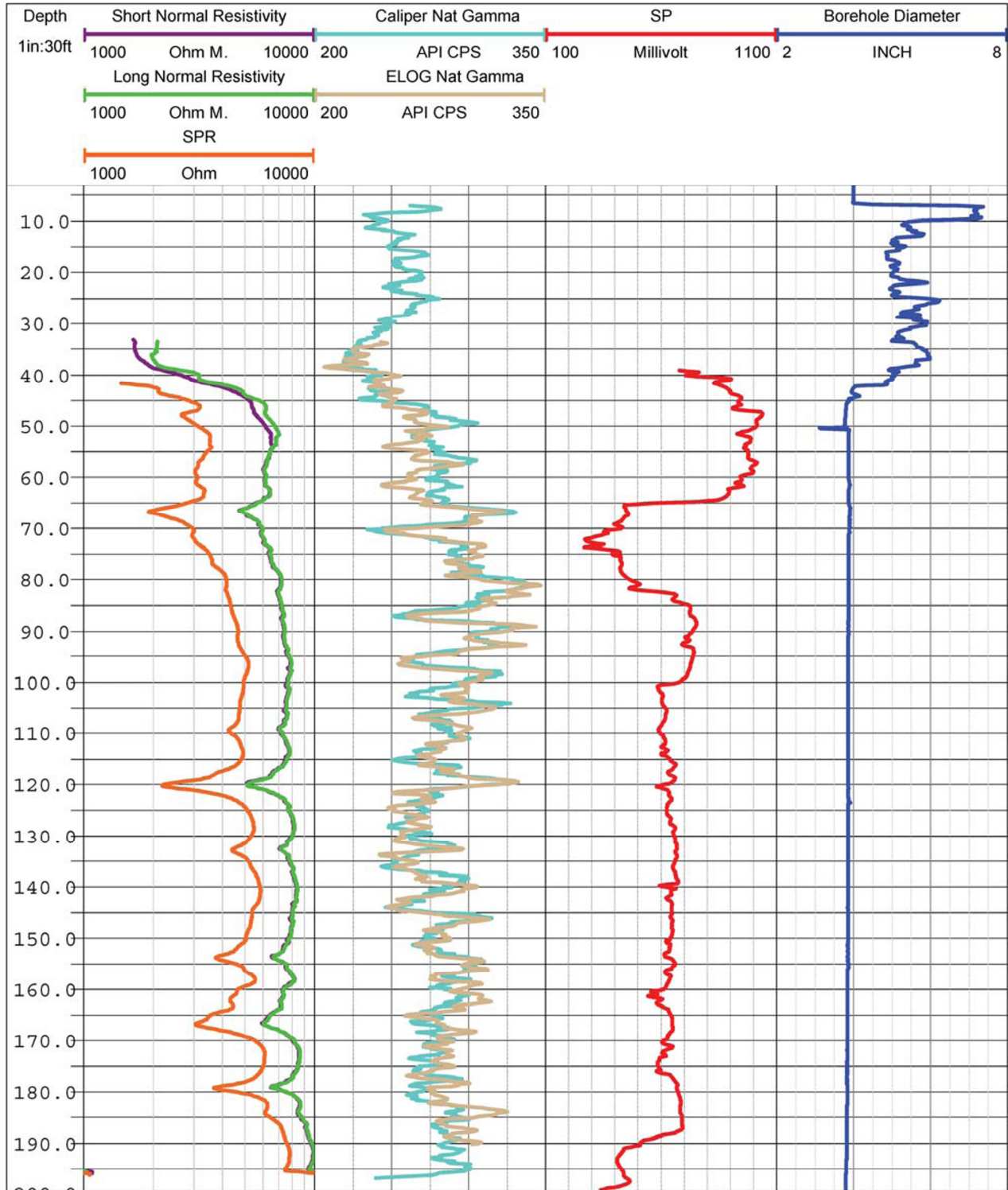


Figure 9. Boring M-30DH, Caliper, Natural gamma, Resistivity and SP logs

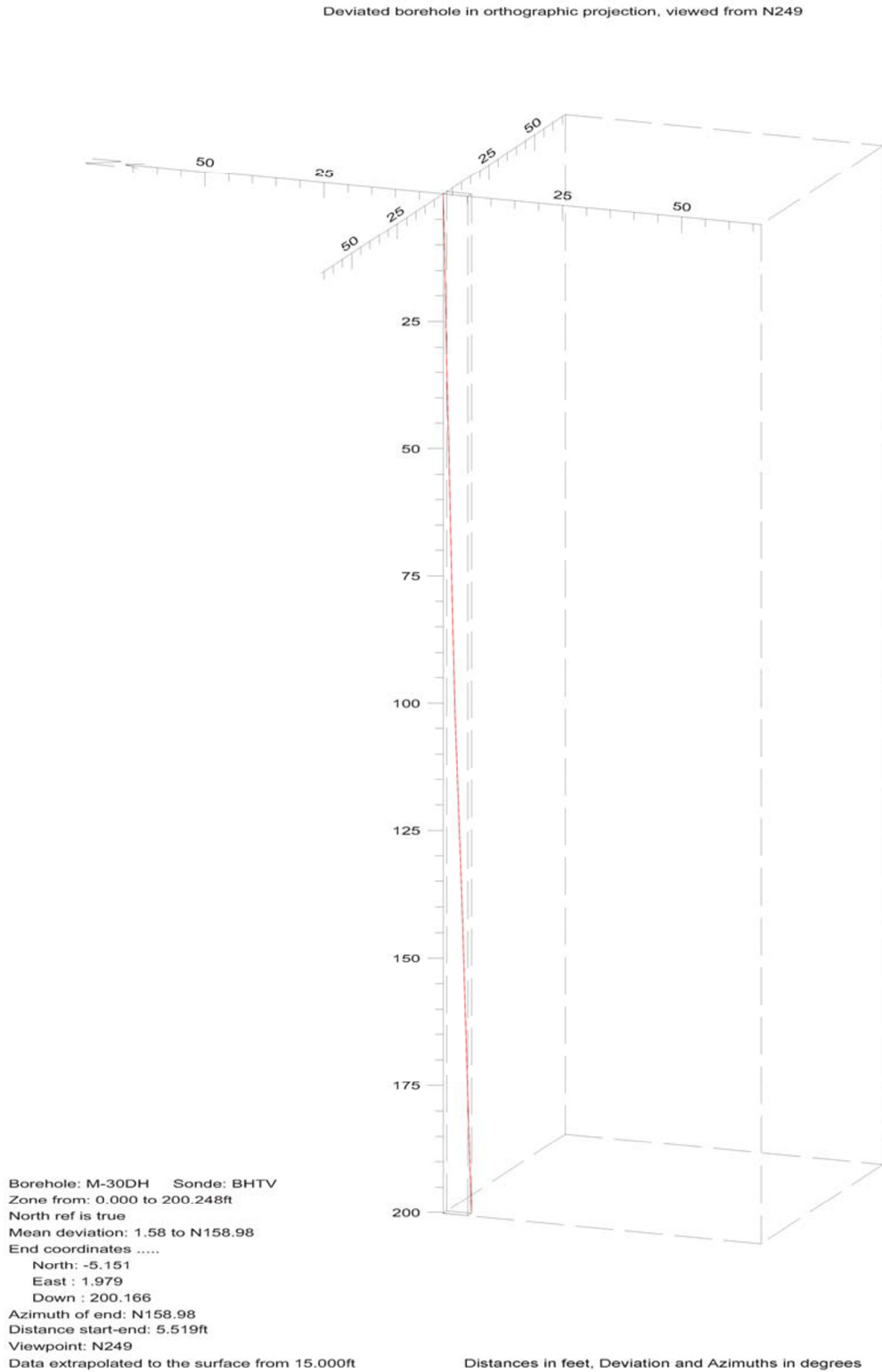


Figure 10. Boring M-30DH, Deviation Projection

**APPENDIX A**

**SUSPENSION VELOCITY MEASUREMENT  
COMPARISON OF SOURCE TO RECEIVER 1  
AND RECEIVER 1 TO RECEIVER 2 ANALYSIS  
RESULTS**

### NORTH ANNA BORING M-10DH Source to Receiver and Receiver to Receiver Analysis

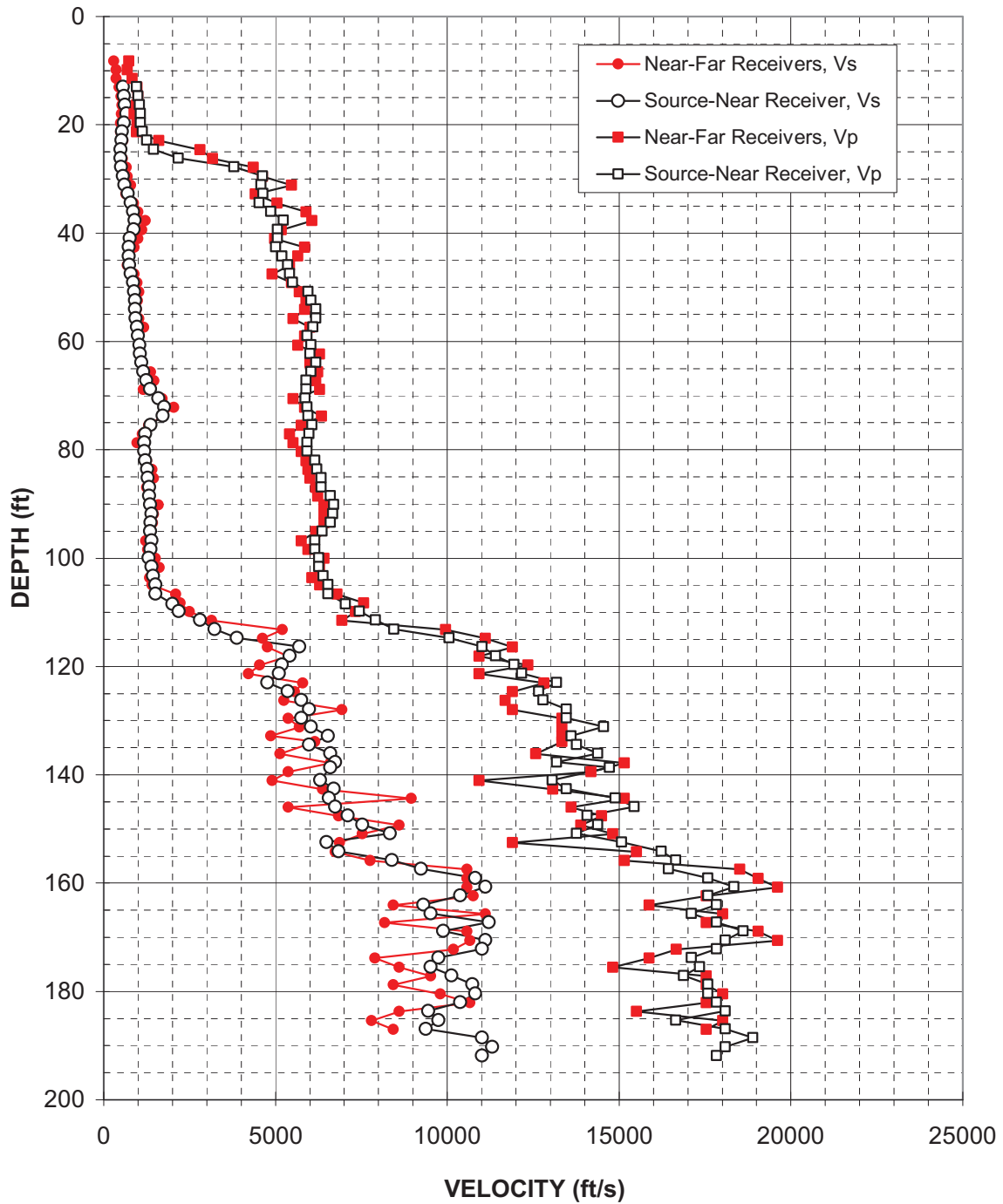


Figure A-1: Boring M-10DH, Suspension S-R1 P- and S<sub>H</sub>-wave velocities

Table A-1. Boring M-10DH, Suspension S-R1 depths and P- and S<sub>H</sub>-wave velocities

**Summary of Compressional Wave Velocity, Shear Wave Velocity, and Poisson's Ratio  
 Based on Source-to-Receiver Travel Time Data - Borehole M-10DH**

American Units			
Depth at Midpoint Between Source and Near Receiver	Velocity		Poisson's Ratio
	V <sub>s</sub>	V <sub>p</sub>	
(ft)	(ft/s)	(ft/s)	
13.0	570	960	0.23
14.7	590	1000	0.23
16.3	620	1040	0.22
18.0	660	1070	0.18
19.6	590	1070	0.28
21.2	540	1130	0.35
22.9	520	1260	0.40
24.5	490	1450	0.44
26.2	490	2170	0.47
27.8	510	3790	0.49
29.4	570	4620	0.49
31.1	600	4590	0.49
32.7	710	4640	0.49
34.4	790	4520	0.48
36.0	860	4870	0.48
37.6	910	5230	0.48
39.3	880	5060	0.48
40.9	760	5060	0.49
42.6	730	5000	0.49
44.2	730	5190	0.49
45.8	750	5360	0.49
47.5	780	5410	0.49
49.1	860	5500	0.49
50.8	890	5940	0.49
52.4	910	6030	0.49
54.0	910	6180	0.49
55.7	920	6180	0.49
57.3	980	6090	0.49
59.0	1000	5920	0.49
60.6	1040	6030	0.48
62.2	1060	6000	0.48
63.9	1100	6180	0.48
65.5	1160	6030	0.48
67.2	1230	5890	0.48
68.8	1360	5890	0.47
70.5	1590	5860	0.46
72.1	1760	5920	0.45
73.7	1720	5940	0.45
75.4	1360	6060	0.47
77.0	1210	5970	0.48

Metric Units			
Depth at Midpoint Between Source and Near Receiver	Velocity		Poisson's Ratio
	V <sub>s</sub>	V <sub>p</sub>	
(m)	(m/s)	(m/s)	
4.0	170	290	0.23
4.5	180	310	0.23
5.0	190	320	0.22
5.5	200	330	0.18
6.0	180	330	0.28
6.5	160	350	0.35
7.0	160	380	0.40
7.5	150	440	0.44
8.0	150	660	0.47
8.5	160	1160	0.49
9.0	170	1410	0.49
9.5	180	1400	0.49
10.0	220	1410	0.49
10.5	240	1380	0.48
11.0	260	1480	0.48
11.5	280	1590	0.48
12.0	270	1540	0.48
12.5	230	1540	0.49
13.0	220	1530	0.49
13.5	220	1580	0.49
14.0	230	1640	0.49
14.5	240	1650	0.49
15.0	260	1680	0.49
15.5	270	1810	0.49
16.0	280	1840	0.49
16.5	280	1880	0.49
17.0	280	1880	0.49
17.5	300	1860	0.49
18.0	310	1800	0.49
18.5	320	1840	0.48
19.0	320	1830	0.48
19.5	340	1880	0.48
20.0	350	1840	0.48
20.5	380	1790	0.48
21.0	410	1790	0.47
21.5	480	1790	0.46
22.0	540	1800	0.45
22.5	530	1810	0.45
23.0	410	1850	0.47
23.5	370	1820	0.48

**Summary of Compressional Wave Velocity, Shear Wave Velocity, and Poisson's Ratio  
 Based on Source-to-Receiver Travel Time Data - Borehole M-10DH**

American Units			
Depth at Midpoint Between Source and Near Receiver	Velocity		Poisson's Ratio
	V <sub>s</sub>	V <sub>p</sub>	
(ft)	(ft/s)	(ft/s)	
78.7	1180	5920	0.48
80.3	1180	5920	0.48
81.9	1220	6150	0.48
83.6	1270	6210	0.48
85.2	1290	6330	0.48
86.9	1320	6330	0.48
88.5	1330	6590	0.48
90.1	1360	6700	0.48
91.8	1400	6660	0.48
93.4	1370	6590	0.48
95.1	1360	6360	0.48
96.7	1400	6150	0.47
98.3	1370	6150	0.47
100.0	1320	6270	0.48
101.6	1400	6270	0.47
103.3	1440	6390	0.47
104.9	1500	6530	0.47
106.5	1510	6530	0.47
108.5	2000	7030	0.46
109.8	2180	7450	0.45
111.5	2800	7910	0.43
113.1	3230	8440	0.41
114.7	3880	10050	0.41
116.4	5700	11010	0.32
118.0	5410	11410	0.35
119.7	5190	11940	0.38
121.3	5100	12170	0.39
122.9	4760	13190	0.43
124.6	5360	12660	0.39
126.2	5750	12790	0.37
127.9	5970	13470	0.38
129.5	5750	13470	0.39
131.1	6030	14550	0.40
132.8	6530	13610	0.35
134.4	5970	13760	0.38
136.1	6590	14390	0.37
137.7	6730	13190	0.32
138.7	6590	14720	0.37
141.0	6300	13050	0.35
142.6	6700	13470	0.34
144.3	6560	14890	0.38
145.9	6730	15440	0.38

Metric Units			
Depth at Midpoint Between Source and Near Receiver	Velocity		Poisson's Ratio
	V <sub>s</sub>	V <sub>p</sub>	
(m)	(m/s)	(m/s)	
24.0	360	1800	0.48
24.5	360	1800	0.48
25.0	370	1870	0.48
25.5	390	1890	0.48
26.0	390	1930	0.48
26.5	400	1930	0.48
27.0	400	2010	0.48
27.5	410	2040	0.48
28.0	430	2030	0.48
28.5	420	2010	0.48
29.0	410	1940	0.48
29.5	430	1870	0.47
30.0	420	1870	0.47
30.5	400	1910	0.48
31.0	430	1910	0.47
31.5	440	1950	0.47
32.0	460	1990	0.47
32.5	460	1990	0.47
33.1	610	2140	0.46
33.5	670	2270	0.45
34.0	850	2410	0.43
34.5	980	2570	0.41
35.0	1180	3060	0.41
35.5	1740	3360	0.32
36.0	1650	3480	0.35
36.5	1580	3640	0.38
37.0	1560	3710	0.39
37.5	1450	4020	0.43
38.0	1640	3860	0.39
38.5	1750	3900	0.37
39.0	1820	4110	0.38
39.5	1750	4110	0.39
40.0	1840	4440	0.40
40.5	1990	4150	0.35
41.0	1820	4190	0.38
41.5	2010	4380	0.37
42.0	2050	4020	0.32
42.3	2010	4490	0.37
43.0	1920	3980	0.35
43.5	2040	4110	0.34
44.0	2000	4540	0.38
44.5	2050	4710	0.38

**Summary of Compressional Wave Velocity, Shear Wave Velocity, and Poisson's Ratio  
 Based on Source-to-Receiver Travel Time Data - Borehole M-10DH**

American Units			
Depth at Midpoint Between Source and Near Receiver	Velocity		Poisson's Ratio
	V <sub>s</sub>	V <sub>p</sub>	
(ft)	(ft/s)	(ft/s)	
147.6	7110	14070	0.33
149.2	7540	14390	0.31
150.8	8330	13760	0.21
152.5	6490	15070	0.39
154.1	6840	16230	0.39
155.8	8380	16660	0.33
157.4	9240	16440	0.27
159.0	10820	17580	0.20
160.7	11110	18350	0.21
162.3	10380	17580	0.23
164.0	9310	17830	0.31
165.6	9520	17110	0.28
167.2	11200	17830	0.17
168.9	9890	18620	0.30
170.5	11110	18090	0.20
172.2	11010	17830	0.19
173.8	9740	17110	0.26
175.4	9520	17340	0.28
177.1	10130	16880	0.22
178.7	10730	17580	0.20
180.4	10820	17580	0.20
182.0	10380	17830	0.24
183.6	9450	18090	0.31
185.3	9740	16660	0.24
186.9	9380	18090	0.32
188.6	11010	18900	0.24
190.2	11300	18090	0.18
191.8	11010	17830	0.19

Metric Units			
Depth at Midpoint Between Source and Near Receiver	Velocity		Poisson's Ratio
	V <sub>s</sub>	V <sub>p</sub>	
(m)	(m/s)	(m/s)	
45.0	2170	4290	0.33
45.5	2300	4380	0.31
46.0	2540	4190	0.21
46.5	1980	4590	0.39
47.0	2090	4950	0.39
47.5	2560	5080	0.33
48.0	2820	5010	0.27
48.5	3300	5360	0.20
49.0	3380	5590	0.21
49.5	3160	5360	0.23
50.0	2840	5430	0.31
50.5	2900	5210	0.28
51.0	3410	5430	0.17
51.5	3010	5670	0.30
52.0	3380	5510	0.20
52.5	3360	5430	0.19
53.0	2970	5210	0.26
53.5	2900	5290	0.28
54.0	3090	5150	0.22
54.5	3270	5360	0.20
55.0	3300	5360	0.20
55.5	3160	5430	0.24
56.0	2880	5510	0.31
56.5	2970	5080	0.24
57.0	2860	5510	0.32
57.5	3360	5760	0.24
58.0	3450	5510	0.18
58.5	3360	5430	0.19

**Notes:**        "-" means no data available at that particular interval of depth.

### NORTH ANNA BORING M-30DH Source to Receiver and Receiver to Receiver Analysis

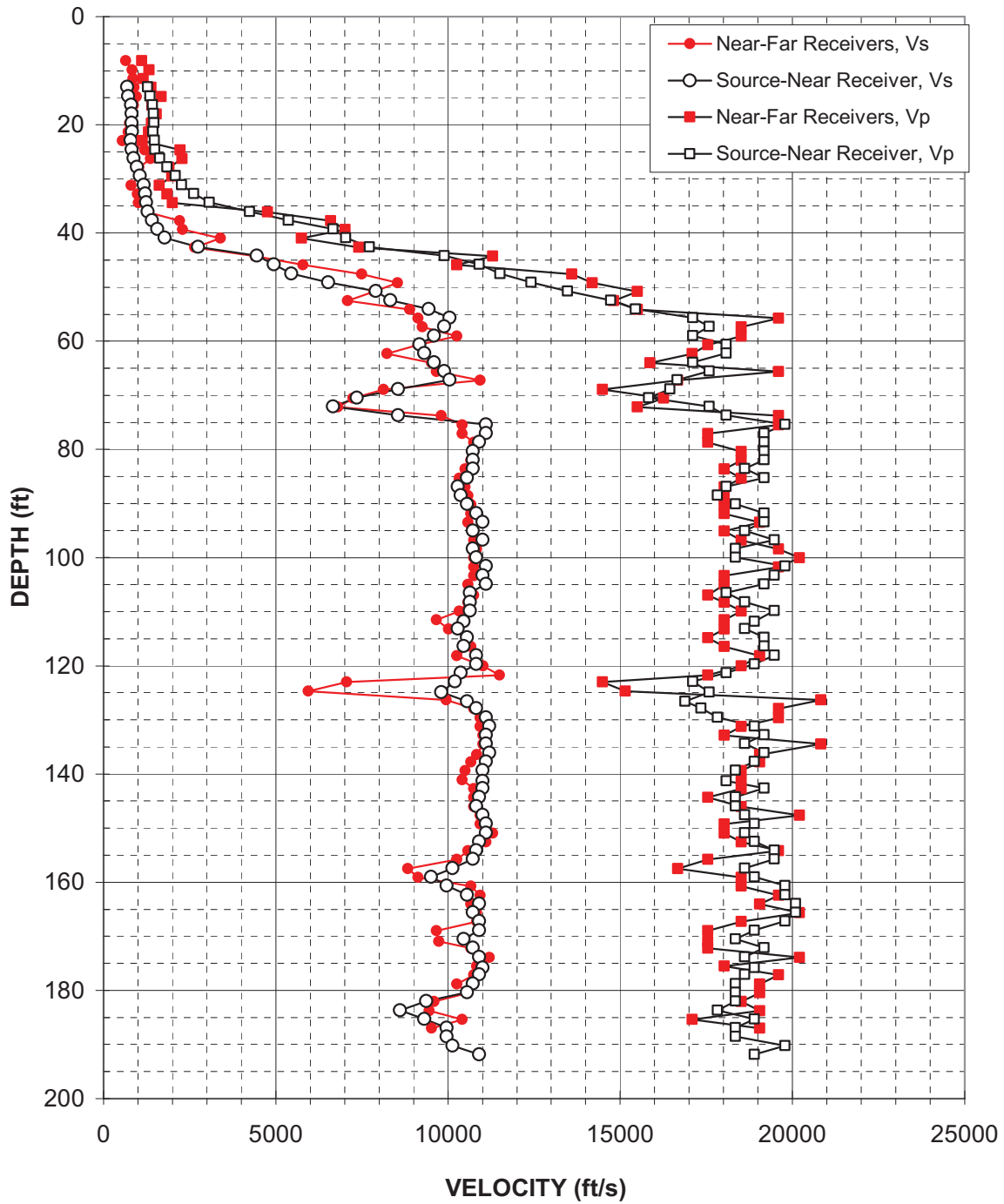


Figure A-2: Boring M-30DH, Suspension S-R1 P- and S<sub>H</sub>-wave velocities

Table A-2. Boring M-30DH, Suspension S-R1 depths and P- and S<sub>H</sub>-wave velocities

**Summary of Compressional Wave Velocity, Shear Wave Velocity, and Poisson's Ratio  
 Based on Source-to-Receiver Travel Time Data - Borehole M-30DH**

American Units			
Depth at Midpoint Between Source and Near Receiver	Velocity		Poisson's Ratio
	V <sub>s</sub>	V <sub>p</sub>	
(ft)	(ft/s)	(ft/s)	
13.0	690	1280	0.30
14.7	720	1350	0.30
16.3	800	1430	0.27
18.0	820	1460	0.27
19.6	820	1470	0.27
21.2	840	1440	0.24
22.9	790	1480	0.30
24.5	820	1500	0.29
26.2	880	1630	0.30
27.8	970	1850	0.31
29.4	1060	2080	0.32
31.1	1170	2270	0.32
32.7	1220	2620	0.36
34.4	1250	3070	0.40
36.0	1280	4250	0.45
37.6	1410	5360	0.46
39.3	1570	6660	0.47
40.9	1780	7030	0.47
42.6	2750	7720	0.43
44.2	4460	9890	0.37
45.8	4950	10910	0.37
47.5	5460	11510	0.35
49.1	6530	12410	0.31
50.8	7910	13470	0.24
52.4	8330	14720	0.26
54.0	9450	15440	0.20
55.7	10050	17110	0.24
57.3	9890	17580	0.27
59.0	9590	17110	0.27
60.6	9170	18090	0.33
62.2	9310	18090	0.32
63.9	9590	17110	0.27
65.5	9890	17580	0.27
67.2	10050	16660	0.21
68.8	8550	16440	0.31
70.5	7360	15830	0.36
72.1	6660	17580	0.42
73.7	8550	18090	0.36
75.4	11110	19780	0.27
77.0	11110	19180	0.25

Metric Units			
Depth at Midpoint Between Source and Near Receiver	Velocity		Poisson's Ratio
	V <sub>s</sub>	V <sub>p</sub>	
(m)	(m/s)	(m/s)	
4.0	210	390	0.30
4.5	220	410	0.30
5.0	240	430	0.27
5.5	250	440	0.27
6.0	250	450	0.27
6.5	260	440	0.24
7.0	240	450	0.30
7.5	250	460	0.29
8.0	270	500	0.30
8.5	300	560	0.31
9.0	320	630	0.32
9.5	360	690	0.32
10.0	370	800	0.36
10.5	380	940	0.40
11.0	390	1290	0.45
11.5	430	1640	0.46
12.0	480	2030	0.47
12.5	540	2140	0.47
13.0	840	2350	0.43
13.5	1360	3010	0.37
14.0	1510	3330	0.37
14.5	1660	3510	0.35
15.0	1990	3780	0.31
15.5	2410	4110	0.24
16.0	2540	4490	0.26
16.5	2880	4710	0.20
17.0	3060	5210	0.24
17.5	3010	5360	0.27
18.0	2920	5210	0.27
18.5	2800	5510	0.33
19.0	2840	5510	0.32
19.5	2920	5210	0.27
20.0	3010	5360	0.27
20.5	3060	5080	0.21
21.0	2610	5010	0.31
21.5	2240	4820	0.36
22.0	2030	5360	0.42
22.5	2610	5510	0.36
23.0	3380	6030	0.27
23.5	3380	5850	0.25

**Summary of Compressional Wave Velocity, Shear Wave Velocity, and Poisson's Ratio  
 Based on Source-to-Receiver Travel Time Data - Borehole M-30DH**

American Units			
Depth at Midpoint Between Source and Near Receiver	Velocity		Poisson's Ratio
	V <sub>s</sub>	V <sub>p</sub>	
(ft)	(ft/s)	(ft/s)	
78.7	10910	19180	0.26
80.3	10730	19180	0.27
81.9	10730	19180	0.27
83.6	10730	18620	0.25
85.2	10550	19180	0.28
86.9	10290	18090	0.26
88.5	10380	17830	0.24
90.1	10550	18350	0.25
91.8	10820	19180	0.27
93.4	11010	19180	0.25
95.1	10730	18620	0.25
96.7	11010	19480	0.27
98.3	10730	18350	0.24
100.0	10820	18350	0.23
101.6	11110	19780	0.27
103.3	11010	19480	0.27
104.9	11110	19180	0.25
106.5	10640	18090	0.24
108.2	10640	18620	0.26
109.8	10640	19480	0.29
111.8	10460	18900	0.28
113.1	10290	18620	0.28
114.7	10550	19180	0.28
116.4	10460	19180	0.29
118.0	10820	19480	0.28
119.7	10820	18900	0.26
121.3	10380	18090	0.25
122.9	10210	17110	0.22
124.9	9810	17580	0.27
126.6	10550	16880	0.18
127.9	10820	17340	0.18
129.5	11110	17830	0.18
131.1	11200	18900	0.23
132.8	11110	19180	0.25
134.4	11110	18620	0.22
136.1	11200	19180	0.24
137.7	11110	18900	0.24
139.3	11010	18350	0.22
141.3	11010	18090	0.21
142.6	11010	19180	0.25
144.3	10910	18350	0.23
145.9	10820	18350	0.23

Metric Units			
Depth at Midpoint Between Source and Near Receiver	Velocity		Poisson's Ratio
	V <sub>s</sub>	V <sub>p</sub>	
(m)	(m/s)	(m/s)	
24.0	3330	5850	0.26
24.5	3270	5850	0.27
25.0	3270	5850	0.27
25.5	3270	5670	0.25
26.0	3220	5850	0.28
26.5	3140	5510	0.26
27.0	3160	5430	0.24
27.5	3220	5590	0.25
28.0	3300	5850	0.27
28.5	3360	5850	0.25
29.0	3270	5670	0.25
29.5	3360	5940	0.27
30.0	3270	5590	0.24
30.5	3300	5590	0.23
31.0	3380	6030	0.27
31.5	3360	5940	0.27
32.0	3380	5850	0.25
32.5	3240	5510	0.24
33.0	3240	5670	0.26
33.5	3240	5940	0.29
34.1	3190	5760	0.28
34.5	3140	5670	0.28
35.0	3220	5850	0.28
35.5	3190	5850	0.29
36.0	3300	5940	0.28
36.5	3300	5760	0.26
37.0	3160	5510	0.25
37.5	3110	5210	0.22
38.1	2990	5360	0.27
38.6	3220	5150	0.18
39.0	3300	5290	0.18
39.5	3380	5430	0.18
40.0	3410	5760	0.23
40.5	3380	5850	0.25
41.0	3380	5670	0.22
41.5	3410	5850	0.24
42.0	3380	5760	0.24
42.5	3360	5590	0.22
43.1	3360	5510	0.21
43.5	3360	5850	0.25
44.0	3330	5590	0.23
44.5	3300	5590	0.23

**Summary of Compressional Wave Velocity, Shear Wave Velocity, and Poisson's Ratio  
 Based on Source-to-Receiver Travel Time Data - Borehole M-30DH**

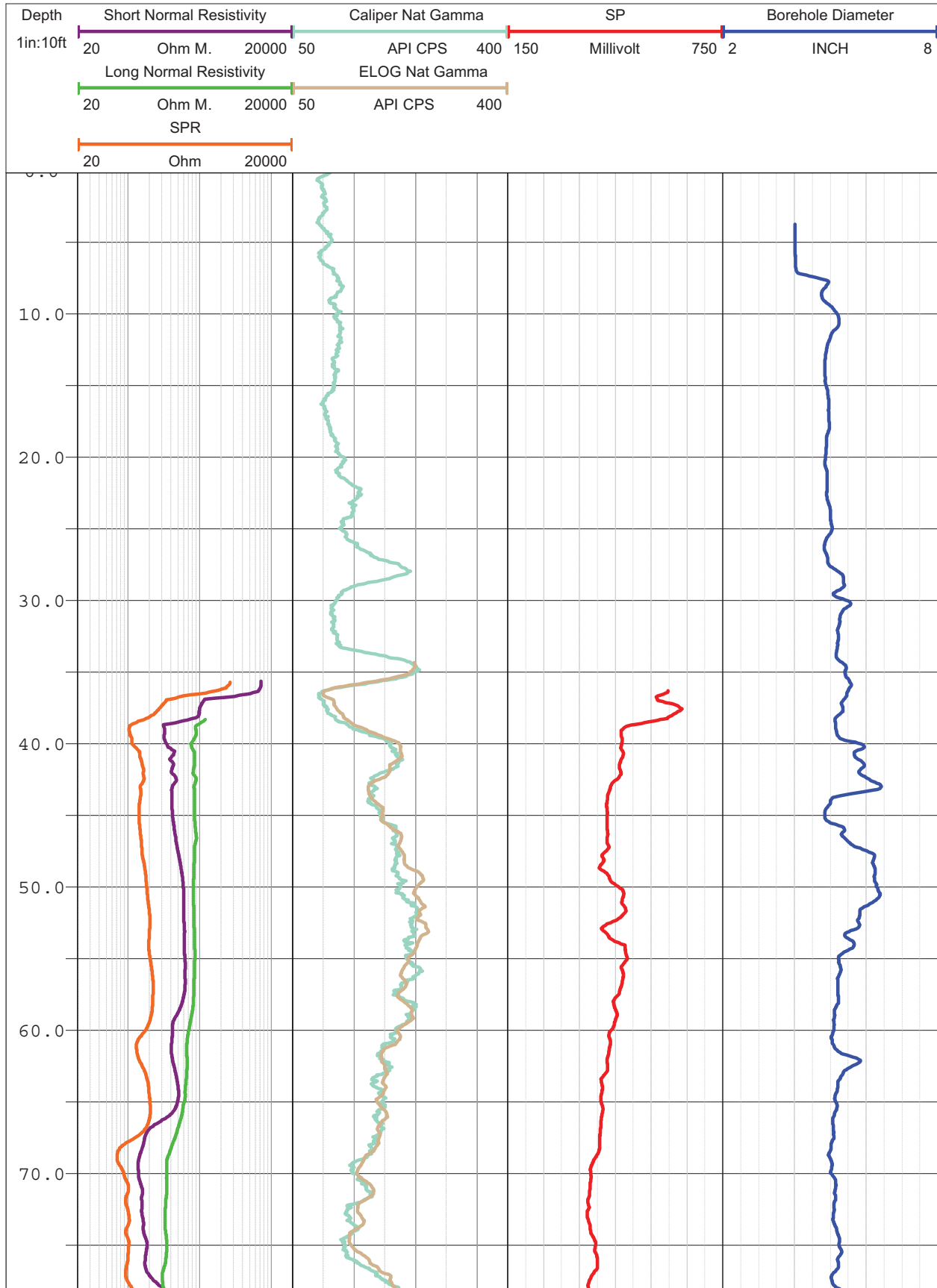
American Units			
Depth at Midpoint Between Source and Near Receiver	Velocity		Poisson's Ratio
	V <sub>s</sub>	V <sub>p</sub>	
(ft)	(ft/s)	(ft/s)	
147.6	11010	18620	0.23
149.2	11110	18900	0.24
150.8	11110	18620	0.22
152.5	10910	18900	0.25
154.1	10820	19480	0.28
155.8	10730	19480	0.28
157.4	10130	18620	0.29
159.0	9520	18900	0.33
160.7	9970	19780	0.33
162.3	10550	19780	0.30
164.0	10910	20100	0.29
165.6	10730	20100	0.30
167.2	10910	19780	0.28
168.9	10910	18900	0.25
170.5	10460	18350	0.26
172.2	10730	19180	0.27
173.8	10910	18620	0.24
175.8	11010	18900	0.24
177.1	10910	18620	0.24
178.7	10730	18350	0.24
180.4	10550	18350	0.25
182.0	9380	18350	0.32
183.6	8610	17830	0.35
185.3	9310	18900	0.34
186.9	9970	18350	0.29
188.6	9970	18350	0.29
190.2	10130	19780	0.32
191.8	10910	18900	0.25

Metric Units			
Depth at Midpoint Between Source and Near Receiver	Velocity		Poisson's Ratio
	V <sub>s</sub>	V <sub>p</sub>	
(m)	(m/s)	(m/s)	
45.0	3360	5670	0.23
45.5	3380	5760	0.24
46.0	3380	5670	0.22
46.5	3330	5760	0.25
47.0	3300	5940	0.28
47.5	3270	5940	0.28
48.0	3090	5670	0.29
48.5	2900	5760	0.33
49.0	3040	6030	0.33
49.5	3220	6030	0.30
50.0	3330	6130	0.29
50.5	3270	6130	0.30
51.0	3330	6030	0.28
51.5	3330	5760	0.25
52.0	3190	5590	0.26
52.5	3270	5850	0.27
53.0	3330	5670	0.24
53.6	3360	5760	0.24
54.0	3330	5670	0.24
54.5	3270	5590	0.24
55.0	3220	5590	0.25
55.5	2860	5590	0.32
56.0	2630	5430	0.35
56.5	2840	5760	0.34
57.0	3040	5590	0.29
57.5	3040	5590	0.29
58.0	3090	6030	0.32
58.5	3330	5760	0.25

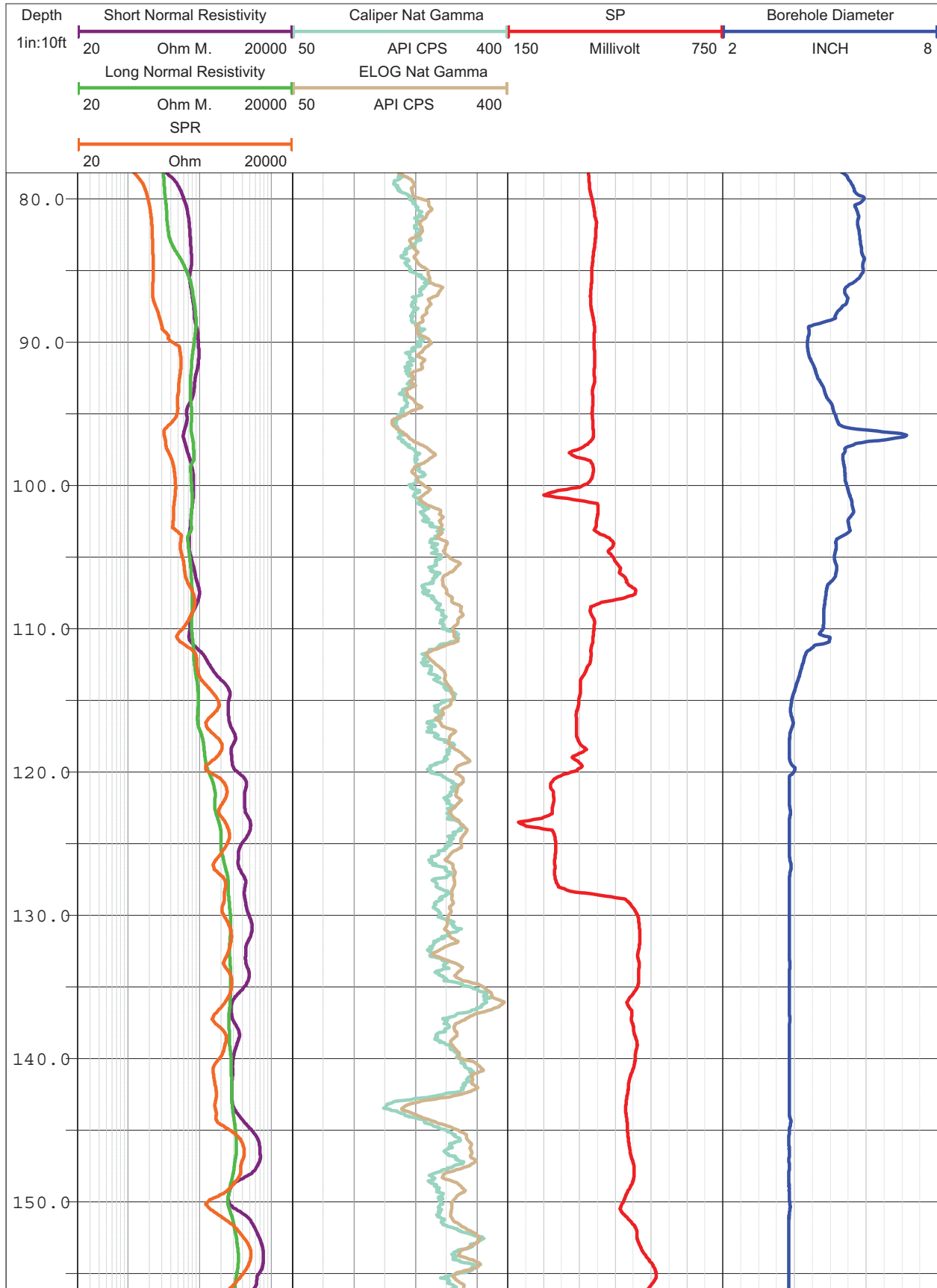
**Notes:**        "-" means no data available at that particular interval of depth.

**APPENDIX B**

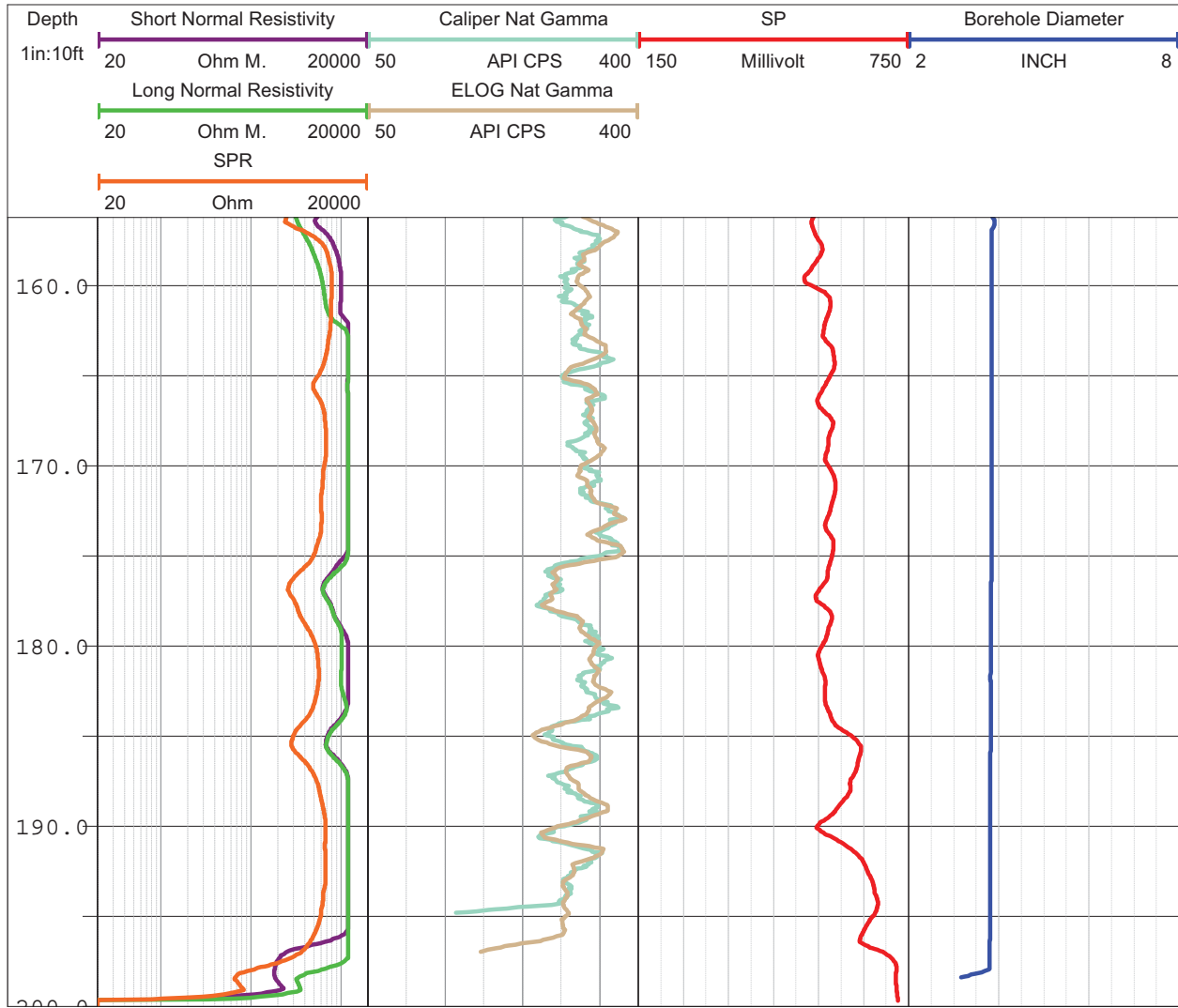
**CALIPER, NATURAL GAMMA, RESISTIVITY,  
AND SPONTANEOUS POTENTIAL LOGS**

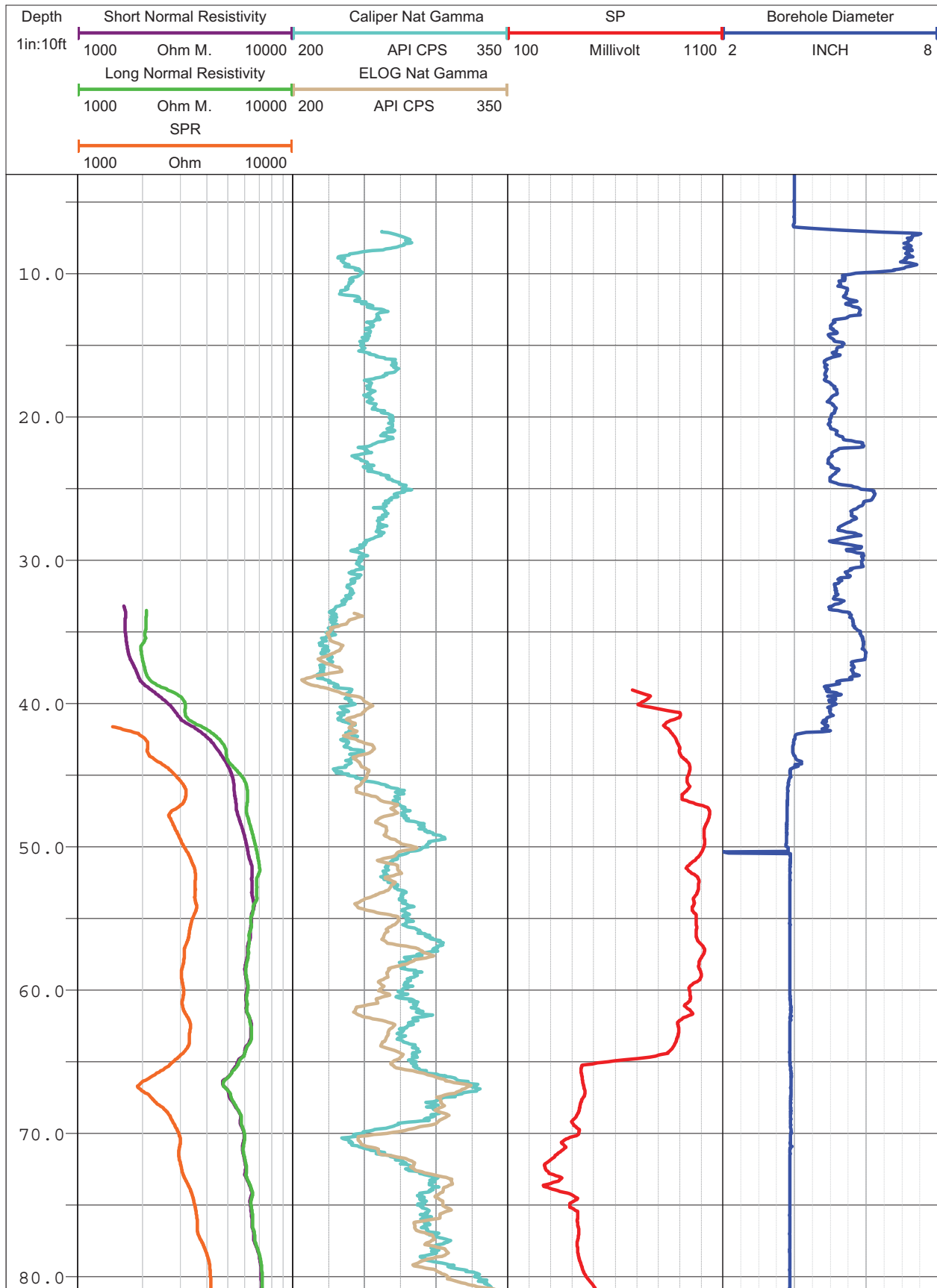


North Anna Boring M-10DH ELOG, Caliper and Natural Gamma rev 1 Sheet 1 of 3

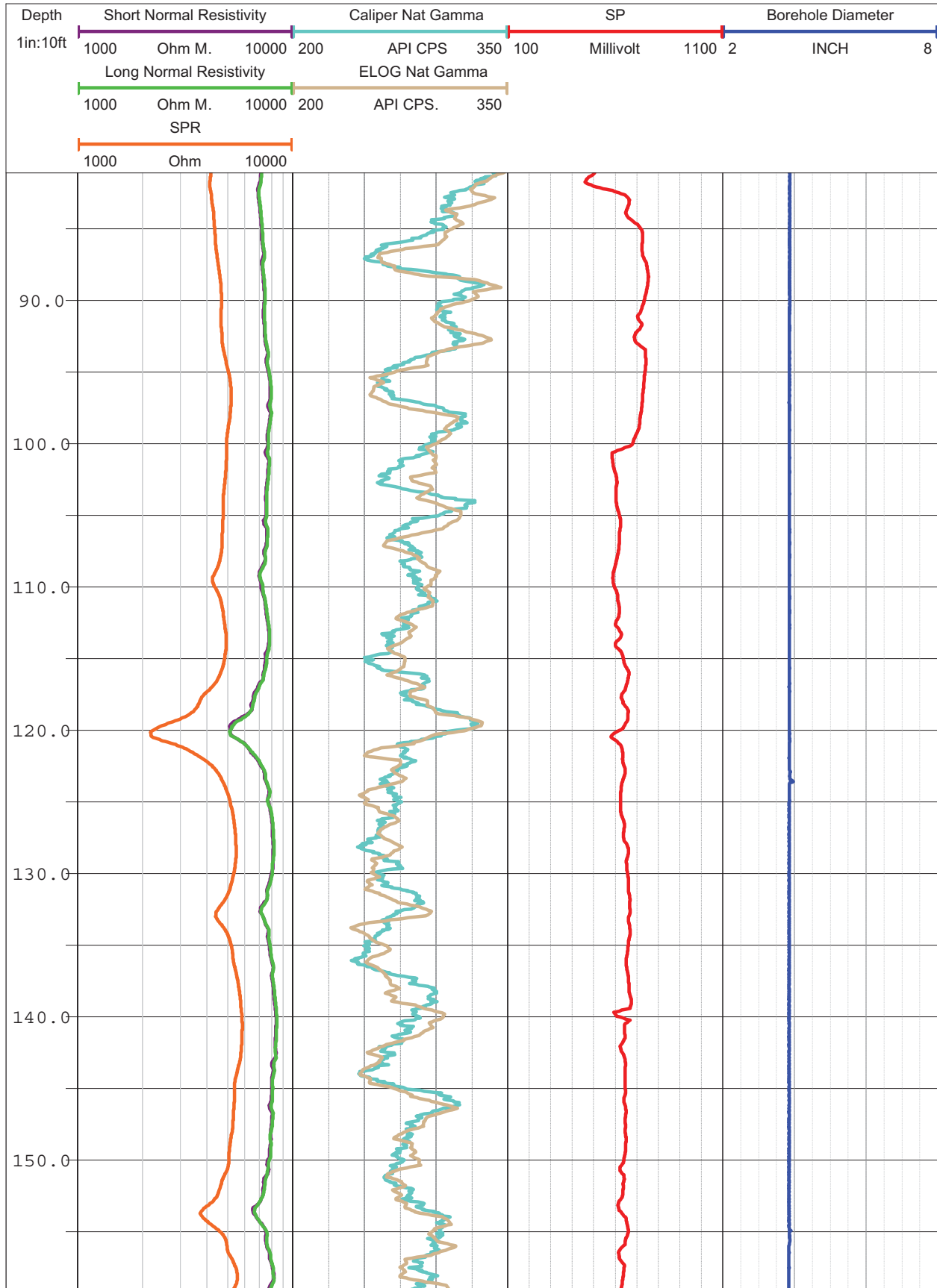


North Anna Boring M-10DH ELOG, Caliper and Natural Gamma rev 1 Sheet 2 of 3





North Anna Boring M-30DH ELOG, Caliper and Natural Gamma rev 1 Sheet 1 of 3



North Anna Boring M-30DH ELOG, Caliper and Natural Gamma rev 1 Sheet 2 of 3

